

Uncertainty Network Risk and Currency Returns

Mykola Babiak*

Lancaster University Management School

Jozef Baruník**

Charles University

First draft: December 2020

This draft: May 16, 2022

Abstract

We examine the pricing of a horizon specific uncertainty network risk, extracted from option implied variances on exchange rates, in the cross-section of currency returns. Buying currencies that are receivers and selling currencies that are transmitters of short-term shocks exhibits a high Sharpe ratio and yields a significant alpha when controlling for standard dollar, carry trade, volatility, variance risk premium and momentum strategies. This profitability stems primarily from the causal nature of shock propagation and not from contemporaneous dynamics. Shock propagation at longer horizons is priced less, indicating a downward-sloping term structure of uncertainty network risk in currency markets.

Keywords: Foreign exchange rates, network risk, currency variance, predictability, term structure

JEL: G12, G15, F31

*Department of Accounting & Finance, Lancaster University Management School, LA1 4YX, UK, E-mail: m.babiak@lancaster.ac.uk.

**Institute of Economic Studies, Charles University, Opletalova 26, 110 00, Prague, CR and Institute of Information Theory and Automation, Academy of Sciences of the Czech Republic, Pod Vodarenskou Vezi 4, 18200, Prague, Czech Republic, E-mail: barunik@utia.cas.cz.

1 Introduction

Countries are connected through a variety of channels including economic activity, trade and financial links among others. Although international connections have been central for understanding market and fundamental macroeconomic risks, the literature has largely ignored the world's largest financial market - the foreign exchange market. In this paper, we explore the properties of a variety of network risk measures in the cross-section of currencies. We document that an uncertainty network strategy, which buys currencies receiving short-term shocks and sells currencies transmitting short-term shocks, generates a high Sharpe ratio and yields a significant alpha when controlling for popular foreign exchange benchmarks. Also, we find that the long-short portfolios based on currency connectedness at longer horizons is less profitable, indicating a downward-sloping term structure of uncertainty network risk in currency markets.¹

We begin by approximating foreign exchange uncertainty through the risk-neutral expectation of the currency variance. The highly liquid and large foreign exchange volatility market provides an excellent opportunity to synthesize such expectations.^{2,3} The data for over-the-counter currency options are available on a daily frequency for a large cross-section of countries. A wide variety of strikes and maturities available on the market allow us to compute the implied variances on exchange rates with precision. Further, the forward-looking nature of currency derivatives, which reflect the expectations of agents about future financial and real macroeconomic risks, is distinct from the backward-looking information extracted from historical price and macroeconomic data.⁴

We continue our empirical investigation by estimating a dynamic horizon specific network among implied variances on exchange rates following the methodology of [Barunik and Ellington \(2020\)](#). The network structure of this paper has several key attributes. First, the connections between two nodes (currencies in our case) are directed, that is, the influence of the currency A on the currency B is not necessarily equal to the impact of the

¹We use the terms network and connectedness interchangeably.

²We follow the model-free approach of [Britten-Jones and Neuberger \(2000\)](#) and [Bakshi, Kapadia, and Madan \(2003\)](#) to compute spot implied variances on exchange rates from currency option prices.

³As of June 2019, a daily average turnover was \$294 billion and a notional amounts outstanding was \$12.7 trillion ([BIS, 2019a,b](#)).

⁴See, for example, [Gabaix and Maggiori \(2015\)](#), [Zviadadze \(2017\)](#), and [Colacito, Croce, Gavazzoni, and Ready \(2018\)](#) for the nature of risks traded in currency markets.

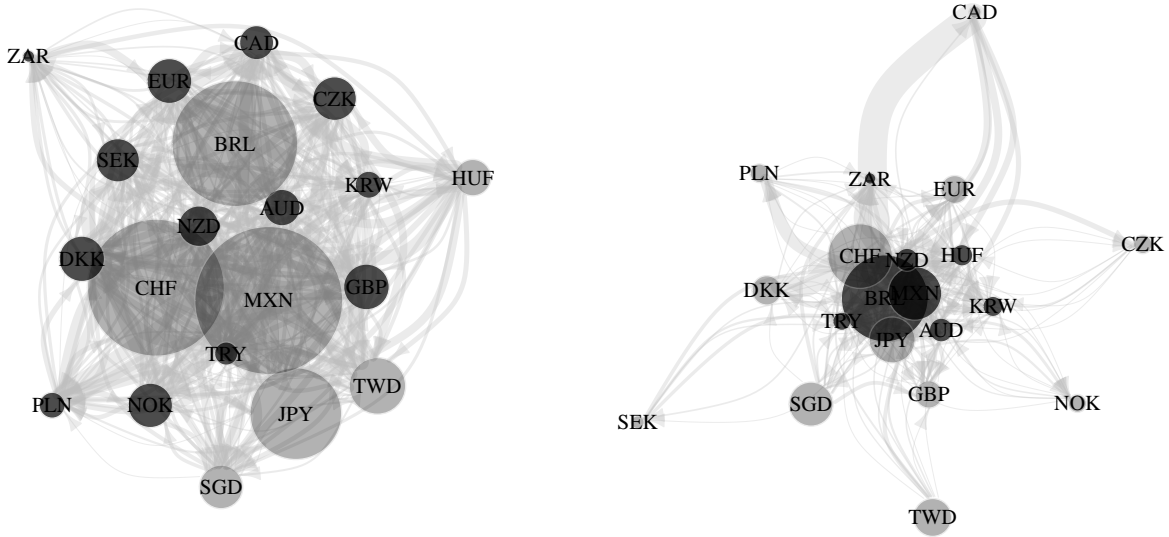


Figure 1. Total and causal short-term currency networks: September 30, 2008

The left (right) figure depicts network connections among currency implied variances based on total (causal) connectedness. Total connectedness measures overall dependencies between currency variances including contemporaneous and causal effects. Causal connectedness is obtained by removing contemporaneous correlations from total connectedness. Arrows denote the direction of connections and the strength of lines denotes the strength of connections. Grey (black) vertices denote currencies receiving (transmitting) more shocks than transmitting (receiving) them. The size of vertices indicates the net-amount of shocks. To enhance readability of plots, the links are drawn if their intensities are greater than a predetermined threshold.

currency B on the currency A. Thus, currency connectedness measures of this paper identify novel links, which are not captured by correlation-based measures. Second, we are able to distinguish between short- and long-term connections among idiosyncratic currency variances and hence we shed light on how connectedness from shocks with different persistence is being priced in currency markets. Third, the international dependencies are naturally driven by contemporaneous fluctuations in global markets and causal influences between countries. In our empirical analysis, we are able to isolate causal connectedness among currency variances by removing contemporaneous correlations. Finally, the network structure is dynamically changing over time, unlike somewhat persistent relationships between countries based on interest rates. Hence, sorting currencies according to the network risk measures is not equivalent, for example, to the currency carry trade.

For twenty countries studied in our paper, Figure 1 depicts total and causal short-term

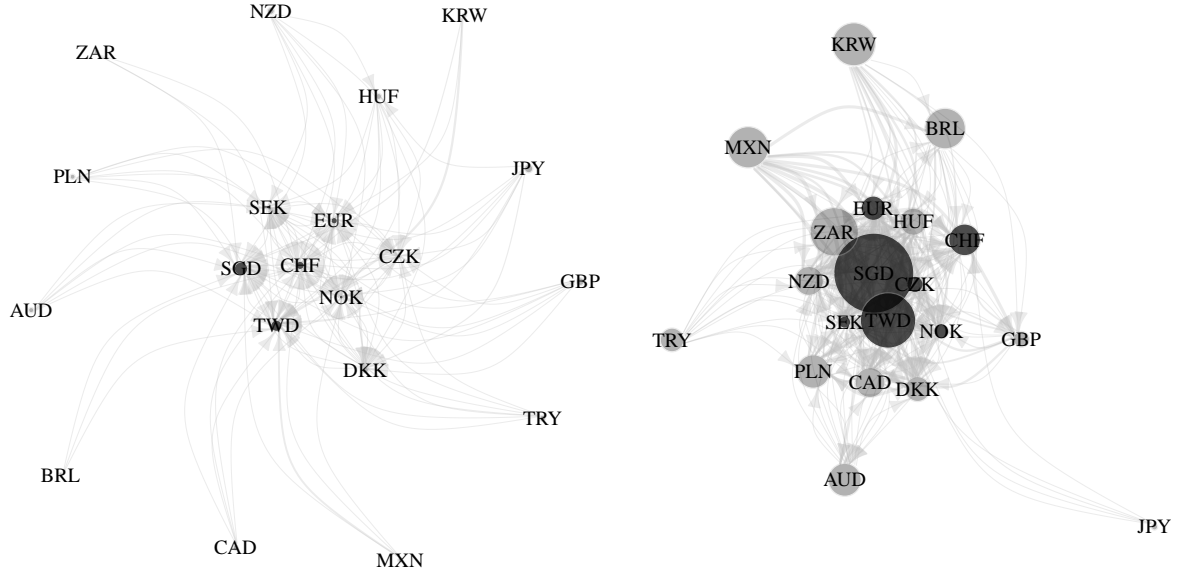


Figure 2. Causal short- and long-term currency networks: August 31, 2011

The left (right) figure depicts short-term (long-term) network connections among currency implied variances based on causal connectedness. Causal connectedness is obtained by removing contemporaneous correlations from total connectedness. Arrows denote the direction of connections and the strength of lines denotes the strength of connections. Grey (black) vertices denote currencies receiving (transmitting) more shocks than transmitting (receiving) them. The size of vertices indicates the net-amount of shocks. To enhance readability of plots, the links are drawn if their intensities are greater than a predetermined threshold.

connections, whereas Figure 2 demonstrates causal links for short- and long-term cases.⁵ The plots show connectedness snapshots during two major recessions (the global financial crisis and the European sovereign debt crisis) and illustrate several interesting features. First, total and causal connections might convey significantly different information about shock propagation in the global currency network. Second, the contribution of short-term and long-horizon connectedness is dynamically changing over time. For example, shortly after the bankruptcy of Lehman Brothers, the market crashes were strongly driven by short-term shocks, whereas fears of contagion in Europe reflect mainly long-term risks. A natural question arises whether this information might be valuable for traders.

We find that uncertainty network does predict currency returns. We build monthly quintile portfolios sorted by the amount of transmitted (received) shocks by each currency to (from) others and also by the difference between transmitted and received shocks.

⁵In the empirical investigation, we define short-term as 1-day to 1-week horizon, medium-term as 1-week to 1-month horizon, and long-term as horizons greater than 1-month.

For portfolio sorting, we use horizon specific total and causal network measures. For instance, for the short-term net-directional (total or causal) network, the first (fifth) portfolio contains the currencies transmitting (receiving) more short-term shocks than receiving (transmitting) them. We document that buying currencies of short-term net-receivers and selling currencies of short-term net-transmitters yields a high Sharpe ratio over the 1996-2013 period (0.65 and 0.80 for total and causal connections). Regressing the excess returns of short-term net-directional portfolios on the dollar, carry trade, volatility, variance risk premium, and momentum strategies yields economically and statistically significant alphas, particularly for a causal connectedness case (6.31% per annum with a t-stat of 3.48). To better understand the sources of this profitability, we sort the currencies into quintiles based on only transmitted or received shocks. The results show that this is the network risk related to transmitting shocks to others, which is strongly priced.

Relative to common currency portfolios, the predictability stemming from causal network risk is primarily driven by changes in exchange rates and not by interest rate differentials. The causal network strategies are also weakly correlated with currency benchmarks, providing excellent diversification gains. The allocation analysis demonstrates that the strategy using causal short-term net-directional connections buys or sells different currencies compared to benchmarks in at least 40% of the time. In contrast, the excess returns of total connectedness portfolios are strongly driven by interest differentials and hence are more correlated with other strategies. The results indicate a distinctive source of causal network returns.

We next focus on the term structure of network risk premia. The profits of net-directional portfolios decrease with the horizon of currency connectedness, suggesting that their expected returns are related to transitory shocks. This result is consistent with the downward sloping term structure of unconditional forward risk premia in equity markets ([Dew-Becker, Giglio, Le, and Rodriguez, 2017](#)). Interestingly, we find that causal to-directional portfolios behave in a strikingly different way. For instance, both average returns and Sharpe ratios of investment strategies focusing only on the amount of transmitted shocks slightly increase with the horizon.

In yet another exercise, we examine whether the excess returns of network-sorted port-

Lustig, Roussanov, and Verdelhan (2011), we perform a principal component decomposition of test assets. The results show that the former cross-section can be summarized by the first two principal components, whereas the latter one requires three components. Motivated by these results, we then formally test a battery of two- and three-factor linear models. None of the pricing kernels including the benchmark currency factors can explain currency returns sorted on total or causal connectedness. In contrast, the corresponding network factor appears to be strongly priced. Finally, for the causal network cross-section, an extended pricing kernel with the dollar, carry trade and network risk factors provides the best-performing three-factor model.

Our empirical evidence is robust to a rich set of robustness checks. First, the magnitude and significance of risk-adjusted and benchmark-adjusted returns of network portfolios monotonically increase when we move to weekly and daily frequencies. Second, the excess returns remain significant after adjusting them for transaction costs using the bid-ask data for exchange rates. Third, the network portfolios generate comparable performance statistics across the first and second half of the total sample.

This paper contributes to the large strand of the literature documenting predictability in currency returns.⁶ The volatility-related strategies exploit global foreign exchange volatility ([Menkhoff, Sarno, Schmeling, and Schrimpf, 2012a](#)) and currency variance risk premium ([Della Corte, Ramadorai, and Sarno, 2016](#)). These strategies can be explained by the models of [Gabaix and Maggiori \(2015\)](#) and [Colacito, Croce, Gavazzeni, and Ready \(2018\)](#). We contribute to this literature by showing how connectedness risk from implied variances on exchange rates is priced in the cross-section of currency excess returns. We demonstrate that network returns stemming from causal nature of shock propagation are virtually unrelated to the existing strategies.

⁶The literature documents the strategies, among many others, based on the carry trade ([Lustig and Verdelhan, 2007](#); [Lustig, Roussanov, and Verdelhan, 2011](#); [Menkhoff, Sarno, Schmeling, and Schrimpf, 2012a](#)), momennum ([Menkhoff, Sarno, Schmeling, and Schrimpf, 2012b](#); [Asness, Moskowitz, and Pedersen, 2013](#); [Dahlquist and Hasseltoft, 2020](#)), business cycles ([Colacito, Riddiough, and Sarno, 2020](#)), and global imbalances ([Corte, Riddiough, and Sarno, 2016](#)).

In related work, [Mueller, Stathopoulos, and Vedolin \(2017\)](#) propose a strategy based on the sensitivity of currencies to the cross-sectional dispersion of conditional foreign exchange correlation. They construct the conditional correlation from spot exchange rates as well as using the currency options for the risk-neutral counterpart. They find some interesting results about the compensation for exposure to high or low dispersion states. In contrast, we focus on dependencies in currency implied variances instead of correlations of spot exchange rates. Furthermore, connectedness measures of our paper are directional unlike correlation-based proxies in [Mueller, Stathopoulos, and Vedolin \(2017\)](#). Further, we are able to disentangle causal from contemporaneous effects in connections between currency variances, which is impossible for correlations in their paper.

Our paper is also related to [Richmond \(2019\)](#) who presents a general equilibrium model explaining the currency carry trade premia by the country's position in the global trade network. Unlike his network risk based on trade linkages, we study the market-based network from currency implied variances. Further, the currency excess returns sorted on network risk measures of our paper are weakly correlated to the standard carry trade. Hence, predictive information of uncertainty network extracted from currency option prices is distinctive from trade links.

Finally, our paper is related to the literature focusing on currency options. [Jurek \(2014\)](#), [Farhi, Fraiberger, Gabaix, Ranciere, and Verdelhan \(2015\)](#) and [Chernov, Graveline, and Zviadadze \(2018\)](#) focus on crash risk in currency markets. Although we use currency options to synthesize implied variances on exchange rates, our main focus is on the properties of network-sorted portfolios, which is different from their papers. Recently, [Della Corte, Kozhan, and Neuberger \(2020\)](#) document a global risk factor in the cross-section of implied volatility returns. The key differentiator of our study from their paper is that we study the network risk premia in the cross-section of spot currency excess returns.

2 Foreign Exchange Uncertainty Network Risk

This section describes the numerical procedure used to measure currency uncertainty network risk. We begin by approximating foreign exchange uncertainty through the risk-neutral expectation of the currency variance that can be synthesized from the quoted currency options. We then provide a general discussion of the econometric methodology used

to estimate a dynamic horizon specific uncertainty network from the currency option implied variances.⁷ We finally discuss a variety of currency uncertainty network risk proxies used in the core analysis.

2.1 Currency Uncertainty: Inferring Investor's Expectations from Option Prices

A natural way to measure uncertainty about future exchange rate fluctuations is through the expectation of the currency variance. To study a network of such expectations in the cross-section of exchange rates, we obtain spot implied variances from OTC currency options by applying a model-free approach of [Britten-Jones and Neuberger \(2000\)](#) and [Bakshi, Kapadia, and Madan \(2003\)](#). Formalizing the discussion, we use prices of European call and put options expiring at time $t + \tau$ to compute the implied variance for an exchange rate k versus the US dollar between two dates t and $t + \tau$:

$$\mathbb{IVar}_t^k = \frac{2}{B^k(t, t + \tau)} \left\{ \int_{F^k(t, t + \tau)}^{\infty} \frac{C^k(t, t + \tau, K)}{K^2} dK + \int_0^{F^k(t, t + \tau)} \frac{P^k(t, t + \tau, K)}{K^2} dK \right\}, \quad (1)$$

where $C^k(t, t + \tau, K)$ and $P^k(t, t + \tau, K)$ denote the prices of call and put contracts at time t with a strike price K and maturity τ , $B^k(t, t + \tau)$ is the price of a country's bond at time t with maturity τ , $F^k(t, t + \tau)$ is the forward exchange rate of the currency k at time t with maturity τ . To compute the model-free implied variances, we discretize the integral in Equation (1) by adopting call and put option prices interpolated around the τ maturity and considering a range of strike prices for the currency k .

2.2 Dynamic Uncertainty Network Risk

Having constructed proxies of forward-looking currency uncertainty, our objective is to define the network for shocks of a specific persistence propagating across the currencies. The knowledge of how a shock to a currency j transmits to a currency k defines a directed link at a given period of time. These disaggregate connections between currency pairs then characterize two major types of network risk: a receiver or a transmitter of shocks. Aggregating the information from all pairs provides a system-wide measure of the forward-looking connectedness among foreign exchanges of countries. In contrast to the network literature in finance ([Elliott, Golub, and Jackson, 2014](#); [Glasserman and](#)

⁷Appendix A provides a detailed description of the estimation procedure used to obtain a dynamic horizon specific uncertainty network risk.

[Young, 2016; Herskovic, 2018](#)), we construct a highly dynamic network encompassing the information for a range of horizons into the future.

A dynamic network can be characterized well through variance decompositions from a time varying parameter vector autoregression (TVP-VAR) approximation model ([Diebold and Yilmaz, 2014](#)). Variance decompositions provide a useful information about how much of the future variance of a variable j is due to shocks in a variable k . The time-varying variance decomposition matrix defines the dynamic network adjacency matrix and is intimately related to network node degrees, mean degrees, and connectedness measures. Further, a frequency domain view on such a network structure allows us to decompose the network to short-, medium- or long-term network risk ([Diebold and Yilmaz, 2014](#)).⁸

Algebraically, the adjacency matrix captures all information about the network, and any sensible measure must be related to it. A typical metric used by the wide network literature that provides the user with information about the relative importance or influence of nodes is network centrality. For our purposes, we want to measure node degrees that capture the number of links to other nodes. The distribution shape of the node degrees is a network-wide property that closely relates to network behavior. As for the connectedness of the network, the location of the degree distribution is key, and hence, the mean of the degree distribution emerges as a benchmark measure of overall network connectedness.

Dynamic horizon specific networks that we work with are more sophisticated than classical network structures. In a typical network, the adjacency matrix contains zero and one entries, depending on the node being linked or not, respectively. In the above notion, one interprets variance decompositions as weighted links showing the strength of the connections. In addition, the links are directed, meaning that the j to k link is not necessarily the same as the k to j link, and hence, the adjacency matrix is not symmetric. These measures are the key to our analysis as directional connectedness risk stems directly from asymmetries within the network.

We construct a dynamic uncertainty network through the TVP-VAR model estimated from currency implied variances following the methodology of [Barunik and Ellington](#)

⁸A natural way to characterize horizon specific dynamics (i.e. short- and long-term) of the dynamic network risk is to consider the spectral representation of the approximating model as recently proposed by [Barunik and Ellington \(2020\)](#).

(2020). We consider a locally stationary TVP-VAR of a lag order p describing the dynamics as:

$$\mathbf{CIV}_{t,T} = \Phi_1(t/T)\mathbf{CIV}_{t-1,T} + \dots + \Phi_p(t/T)\mathbf{CIV}_{t-p,T} + \epsilon_{t,T}, \quad (2)$$

where $\mathbf{CIV}_{t,T} = \left(\mathbf{CIV}_{t,T}^{(1)}, \dots, \mathbf{CIV}_{t,T}^{(N)} \right)^\top$ is a doubly indexed N -variate time series of currency variances, $\epsilon_{t,T} = \Sigma^{-1/2}(t/T)\boldsymbol{\eta}_{t,T}$, $\boldsymbol{\eta}_{t,T} \sim NID(0, \mathbf{I}_M)$ and $\Phi(t/T) = (\Phi_1(t/T), \dots, \Phi_p(t/T))^\top$ are the time varying autoregressive coefficients. Note that t refers to a discrete time index $1 \leq t \leq T$ and T is an additional index indicating the sharpness of the local approximation of the time series by a stationary process. Rescaling time such that the continuous parameter $u \approx t/T$ is a local approximation of the weakly stationary time-series (Dahlhaus, 1996), we approximate $\mathbf{CIV}_{t,T}$ in a neighborhood of $u_0 = t_0/T$ by a stationary process:

$$\widetilde{\mathbf{CIV}}_t(u_0) = \Phi_1(u_0)\widetilde{\mathbf{CIV}}_{t-1}(u_0) + \dots + \Phi_p(u_0)\widetilde{\mathbf{CIV}}_{t-p}(u_0) + \epsilon_t. \quad (3)$$

The TVP-VAR process has a time varying Vector Moving Average VMA(∞) representation (Dahlhaus, Polonik, et al., 2009; Barunik and Ellington, 2020):

$$\mathbf{CIV}_{t,T} = \sum_{h=-\infty}^{\infty} \Psi_{t,T}(h)\epsilon_{t-h} \quad (4)$$

where parameter vector $\Psi_{t,T}(h) \approx \Psi(t/T, h)$ is a time varying impulse response function characterized by a bounded stochastic process.⁹ Information contained in $\Psi_{t,T}(h)$ permits the measurement of the contribution of shocks in the system. Hence, its transformations over time will determine the network risk. Since a shock to a variable in the model does not necessarily appear alone, an identification scheme is crucial in identifying the network. We adapt the generalized identification scheme of Pesaran and Shin (1998), with its extension to locally stationary process by Barunik and Ellington (2020).

We transform local impulse responses in the system to local impulse transfer functions using Fourier transformations. This allows us to measure the horizon specific dynamics of network based on heterogeneous persistence of shocks in the system. A dynamic representation of the variance decomposition of shocks from asset j to asset k then establishes dynamic horizon specific adjacency matrix, which is central to our uncertainty network

⁹Since $\Psi_{t,T}(h)$ contains an infinite number of lags, we approximate the moving average coefficients at $h = 1, \dots, H$ horizons.

risk measures.

Specifically, the element of such a matrix, which captures how shocks from a currency j are propagated to a currency k at a given point of time $u = t_0/T$ and a given horizon $d_i \in \mathcal{H} = \{\mathcal{S}, \mathcal{M}, \mathcal{L}\}$, is formally defined as:

$$[\theta(u, d_i)]_{j,k} = \frac{\widehat{\sigma}_{kk}^{-1} \sum_{\omega \in d_i} \left([\widehat{\Psi}(u, \omega) \widehat{\Sigma}(u)]_{j,k} \right)^2}{\sum_{\omega \in \mathcal{H}} [\widehat{\Psi}(u, \omega) \widehat{\Sigma}(u) \widehat{\Psi}^\top(u, \omega)]_{j,j}}, \quad (5)$$

where $\widehat{\Psi}(u, \omega) = \sum_{h=0}^{H-1} \sum_h \widehat{\Psi}(u, h) e^{-i\omega h}$ is an impulse transfer function estimated from Fourier frequencies ω of impulse responses that cover a specific horizon d_i frequencies.¹⁰ It is important to note that $[\theta(u, d)]_{j,k}$ is a natural disaggregation of traditional variance decompositions to a time-varying and h -horizon adjacency matrix. This is because the portion of the local error variance of the j -th variable at horizon h due to shocks in the k -th variable is scaled by the total variance of the j -th variable. As the rows of the dynamic adjacency matrix do not necessarily sum to one, we normalize the element in each by the corresponding row sum: $[\widetilde{\theta}(u, d)]_{j,k} = [\theta(u, d)]_{j,k} / \sum_{k=1}^N [\theta(u, d)]_{j,k}$. Equation (5) defines a dynamic horizon specific network risk completely. Naturally, our adjacency matrix is filled with weighted links showing strengths of the connections. The links are directional, meaning that the j to k link is not necessarily the same as the k to j link. In sum, the adjacency matrix is asymmetric, horizon specific and evolves dynamically.

To obtain the time-varying coefficient estimates $\widehat{\Phi}_1(u), \dots, \widehat{\Phi}_p(u)$ and the time-varying covariance matrix $\widehat{\Sigma}(u)$ at a given point of time $u = t_0/T$, we estimate the approximating model in Equation (3) using Quasi-Bayesian Local-Likelihood (QBLL) methods (Petrova, 2019). Specifically, we use a kernel weighting function, which puts larger weights to those observations surrounding the period whose coefficient and covariance matrices are of interest. Using conjugate priors, the (quasi) posterior distribution of the parameters of the model are available analytically. This alleviates the need to use a Markov Chain Monte Carlo (MCMC) simulation algorithm and permits the use of parallel computing. We provide a detailed discussion of the estimation algorithm in Appendix A.

¹⁰Note that $i = \sqrt{-1}$.

Finally, the variance decompositions of the forecast errors from the $VMA(\infty)$ representation require a truncation of the infinite horizon with a H horizon approximation. As $H \rightarrow \infty$ the error disappears (Lütkepohl, 2005). We note here that H serves as an approximating factor and has no interpretation in the time-domain. We obtain horizon specific measures using Fourier transforms and set our truncation horizon $H=100$; results are qualitatively similar for $H \in \{50, 100, 200\}$.

2.3 Total and Causal Effects: Removing Contemporaneous Correlations

An important feature we focus on is a direct causal interpretation of our network risk measures. Rambachan and Shephard (2019) provide a general discussion about causal interpretation of impulse response analysis in the time series literature. In particular, they argue that if an observable time series is shown to be a *potential outcome* time series, then generalized impulse response functions have a direct causal interpretation. Potential outcome series describe the output for a particular path of treatments at time t .

In the context of our study, paths of treatments are shocks. The assumptions required for a potential outcome series are natural and intuitive for a time series of currencies: i) they depend only on past and current shocks; ii) series are outcomes of shocks; and iii) assignments of shocks depend only on past outcomes and shocks. The dynamic adjacency matrix we use above to characterize the currency network risk is a transformation of generalized impulse response functions. Therefore, the adjacency matrix and all measures that stem from manipulations of its elements possess a causal interpretation; thus establishing the notion of causal dynamic network measures.

In computing our measures, we also diagonalize the covariance matrix because our objective is to focus on the causal affects of network connections. The $\Psi(u, d)$ matrix embeds the causal nature of network linkages, and the covariance matrix $\Sigma(u)$ contains contemporaneous covariances within the off-diagonal elements. By diagonalizing the covariance matrix, we remove the contemporaneous effects and focus solely on causation. Hence, the measures introduced in the next section will be applied to total and causal linkages depending on whether we include or exclude contemporaneous correlations.

2.4 Uncertainty Network Risk Measures

To evaluate the uncertainty network risk from the estimated model, we use several definitions that focus on aggregate characteristics as well as disaggregate connections between currencies. We focus on measures revealing when an individual currency is a transmitter or a receiver of shocks.

First, horizon-specific from-directional network risk, which measures how much of each currency's j variance is due to shocks of other currencies $j \neq k$ in the cross-section, is defined as:

$$\mathcal{F}_{j \leftarrow \bullet}(u, d) = \sum_{\substack{k=1 \\ k \neq j}}^N \left[\tilde{\theta}(u, d) \right]_{j,k} \quad d \in \mathcal{H} = \{\mathcal{S}, \mathcal{M}, \mathcal{L}\}. \quad (6)$$

Second, horizon-specific to-directional network risk, which measures the contribution of each currency's j variance to variances of other currencies in the cross-section, is given by:

$$\mathcal{T}_{j \rightarrow \bullet}(u, d) = \sum_{\substack{k=1 \\ k \neq j}}^N \left[\tilde{\theta}(u, d) \right]_{k,j} \quad d \in \mathcal{H} = \{\mathcal{S}, \mathcal{M}, \mathcal{L}\}. \quad (7)$$

One can interpret these measures as dynamic to-degrees and from-degrees that associate with the nodes of weighted directed network captured by a variance decomposition matrix. These two measures show how other currencies contribute to the risk of a currency j , and how a currency j contributes to the riskiness of others, respectively, in a time-varying fashion at a horizon d . One can simply add these measures across all horizons to obtain total time-varying measures:

$$\mathcal{F}_{j \leftarrow \bullet}(u, \mathcal{T}) = \sum_{d \in \{\mathcal{S}, \mathcal{M}, \mathcal{L}\}} \mathcal{F}_{j \leftarrow \bullet}(u, d) \quad \wedge \quad \mathcal{T}_{j \rightarrow \bullet}(u, \mathcal{T}) = \sum_{d \in \{\mathcal{S}, \mathcal{M}, \mathcal{L}\}} \mathcal{T}_{j \rightarrow \bullet}(u, d) \quad (8)$$

Third, combining two notions of receivers and transmitters of shocks presented above, we define a horizon specific net-directional network risk:

$$\mathcal{N}_{j \rightarrow \bullet}(u, d) = \mathcal{T}_{j \rightarrow \bullet}(u, d) - \mathcal{F}_{j \leftarrow \bullet}(u, d) \quad d \in \mathcal{H} = \{\mathcal{S}, \mathcal{M}, \mathcal{L}, \mathcal{T}\}. \quad (9)$$

In conclusion, we aim to study the properties of to-, from- and net-directional network portfolios sorted by the corresponding network risk proxies defined by Equations (6)-(9). Furthermore, each portfolio group is constructed using total and causal network linkages

as discussed in Section 2.3.

3 Data and Currency Portfolios

3.1 *Currency Options Data*

We start our empirical investigation by collecting daily OTC option implied volatilities on exchange rates versus the US dollar from JP Morgan and Bloomberg. Following [Della Corte, Ramadorai, and Sarno \(2016\)](#) and [Della Corte, Kozhan, and Neuberger \(2020\)](#), we consider a sample of the following 20 developed and emerging market countries: Australia, Brazil, Canada, Czech Republic, Denmark, Euro Area, Hungary, Japan, Mexico, New Zealand, Norway, Poland, Singapore, South Africa, South Korea, Sweden, Switzerland, Taiwan, Turkey, and United Kingdom. The data cover the sample period from January 1996 to December 2013. The cross-section of currencies starts with 10 countries at the beginning and gradually increases over time, with implied volatilities on all exchange rates being available from 2004 until the end of the sample in 2013.¹¹

We synthesize spot implied variances using a model free approach of [Britten-Jones and Neuberger \(2000\)](#), which requires currency option prices for a range of strike prices. Quotes for OTC currency options are expressed in terms of [Garman and Kohlhagen \(1983\)](#) implied volatilities for selected combinations of plain-vanilla options (at-the-money, 10 and 25 delta put and call options). We recover strike prices from deltas and option prices from implied volatilities by employing interest rates from Bloomberg and spot and forward exchange rates from Barclays and Reuters via Datastream. Using this recovery procedure, we obtain plain vanilla European calls and puts for exchange rates versus the US dollar for a range of maturities: 1 month, 3 months, 6 months, 12 months, and 24 months.

Since our investment strategy is carried out at the monthly frequency, it is natural to assume that traders prefer to employ the 1-month spot implied variances on exchange rates for detecting uncertainty network risk instead of using data for longer maturities. We therefore work with the spot 1-month variances on currencies in our empirical analysis. Further, we construct currency connectedness measures using the variances at the daily frequency to increase the number of observations in our estimation procedure and ultimately to better capture the dynamic nature of uncertainty network risk. We then fil-

¹¹We greatly appreciate help of Roman Kozhan with the currency option data.

ter end-of-month estimates of how currencies are connected to each other to construct the long-short network portfolios.

3.2 Exchange Rate Data

We retrieve daily bid, mid, and ask spot and forward exchange rates versus the US dollar from Barclays and Reuters via Datastream. We further obtain daily nominal interest rates for domestic (the US in our case) and foreign countries from Bloomberg. The core empirical analysis is conducted at the monthly frequency and hence we sample end-of-month observations of all time series. We match exchange and interest rate data with currency option data for the cross-section of 20 countries and the sample period from January 1996 to December 2013 as described above.

3.3 Currency Excess Returns

We denote spot and forward exchange rate of foreign currency k at time t as S_t^k and F_t^k . Exchange rates are expressed in units of foreign currency per US dollar. Thus, an increase in S_t^k indicates a depreciation of the foreign currency. Following [Menkhoff, Sarno, Schmeling, and Schrimpf \(2012a\)](#), we define one-period ahead excess return to a US investor for holding foreign currency k at time t as

$$rx_{t+1}^k = i_t^k - i_t - \Delta s_{t+1}^k \approx f_t^k - s_{t+1}^k, \quad (10)$$

in which i_t^k and i_t represent the risk-less rates of the foreign country k and the US, Δs_{t+1}^k is the log change in the spot exchange rate, f_t^k and s_{t+1}^k denote the log spot and forward rates. Under covered interest rate parity (CIP), the interest rate differential $i_t^k - i_t$ is equal to forward discount $f_t^k - s_t^k$. Thus, the approximation in Equation (10) states that the excess currency return equals the difference between the current forward rate and future spot rate. The early literature documented that CIP held even for very short horizons ([Akram, Rime, and Sarno, 2008](#)), while recent evidence has shown CIP deviations in the post global financial crisis period ([Du, Tepper, and Verdelhan, 2018](#); [Andersen, Duffie, and Song, 2019](#)). We demonstrate that the profitability of uncertainty network strategies studied in our paper stems primarily from spot exchange rate predictability. Therefore, our key results do not depend on the validity of the CIP condition.

3.4 Uncertainty Network Portfolios

The measures of network connectedness among exchange rate implied variances capture multiple risks that could be important for investors forming currency portfolios. First, unlike the previous literature focusing on the correlation risk in currency returns, the network risk proxies of our paper can identify the causal nature of network linkages by removing the contemporaneous effects. Thus, we are able to detect novel risks originating from the causal propagation of shocks in the cross-section of exchange rates. Second, using individual connections between exchange rates, we can quantify the aggregate amount of shocks that a particular currency transmits to or receives from others. Similarly, we can compute the net-directional connectedness measure by taking the difference between shocks that are transmitted and received. Third, a large strand of the literature studies the role of shocks with different persistence. For instance, long-term fluctuations in expected growth and volatility of cash-flows (Bansal and Yaron, 2004) have played a central role for understanding equity, bond, and currency returns. Our econometric methodology allows us to disentangle the effect of a horizon specific network risk. We therefore can shed light on the term structure of forward-looking uncertainty connectedness in the cross-section of currencies. In sum, we construct a battery of portfolios based on a variety of network connectedness measures to quantitatively evaluate which network risks are priced in currency markets.

Specifically, at the end of each time period t (the last day of the month in the core analysis), we sort currencies into five portfolios using one of network measures constructed and described in Section 2.4. The first quintile portfolio \mathcal{P}_1 comprises 20% of all currencies with the highest values of a particular network characteristic, whereas the fifth quintile portfolio \mathcal{P}_5 contains 20% of all currencies with the lowest values. Each \mathcal{P}_i is an equally weighted portfolio of the corresponding currencies. We next form a long-short strategy that buys \mathcal{P}_5 and sells \mathcal{P}_1 .

We report the results for five quintile portfolios and a long-short strategy sorted by (i) short- (\mathcal{S}), medium- (\mathcal{M}), and long-term (\mathcal{L}) as well as total (\mathcal{T}) net-directional connectedness constructed from total (contemporaneous and causal) and only causal (excluding contemporaneous) linkages. The corresponding zero-cost strategies are denoted by $\mathcal{N}(\mathcal{H})$ where $\mathcal{H} \in \{\mathcal{S}, \mathcal{M}, \mathcal{L}, \mathcal{T}\}$. We additionally dissect the sources of profitability of

net-directional network strategies by solely looking at the risk of being a transmitter or a receiver of shocks. In particular, we construct the portfolios based on (ii) to-directional and (iii) from-directional connectedness measures. Similarly to the portfolios in (i), we report the results for all horizons considered, but for the sake of a convenient illustration we focus on the case with causal linkages.¹² The respective to-directional and from-directional long-short portfolios are denoted by $\mathcal{T}(\mathcal{H})$ and $\mathcal{F}(\mathcal{H})$ where $\mathcal{H} \in \{\mathcal{S}, \mathcal{M}, \mathcal{L}, \mathcal{T}\}$.

3.5 *Dollar and Carry Trade Strategies*

We compare the performance of network-sorted portfolios to standard investment strategies from the existing literature. Following [Lustig, Roussanov, and Verdelhan \(2011\)](#), we build a portfolio that is the average of all currencies available in a particular time period. The resulting returns are equivalent to borrowing money in the US and investing in global money markets outside the US. This zero-cost strategy is commonly called the dollar risk factor or the dollar portfolio (dol). Further, we sort all currencies available at time t into five quintile portfolios on the basis of their interest rate differential (or forward premia) relative to the US. The first quintile portfolio \mathcal{P}_1 comprises 20% of all currencies with the highest interest rates, whereas the fifth quintile portfolio \mathcal{P}_5 contains 20% of all currencies with the lowest interest rates. The difference between \mathcal{P}_1 and \mathcal{P}_5 is called the carry trade strategy (car), which is equivalent to borrowing money in low interest rate countries and investing in high interest rate countries.

3.6 *Volatility Portfolios*

We create a tradable strategy taking into account past realized volatility of currencies in the spirit of [Menkhoff, Sarno, Schmeling, and Schrimpf \(2012a\)](#). At the end of each month t , we compute the square root of the sum of squared daily log exchange rate returns during the current month. We sort all currencies available at time t into five quintile portfolios on the basis of their monthly realized volatility. The first quintile portfolio \mathcal{P}_1 comprises 20% of all currencies with the highest volatility, whereas the fifth quintile portfolio \mathcal{P}_5 contains 20% of all currencies with the lowest volatility. The difference between \mathcal{P}_1 and \mathcal{P}_5 is called the volatility strategy (vol), which is equivalent to selling low volatility risk countries and buying high volatility risk countries.

¹²The results of quintile and zero-cost portfolios sorted on to- and from-directional connections with total linkages are available upon request.

3.7 Variance Risk Premium Portfolios

We construct an investment strategy reflecting the costs of insuring currency variance risk that has been recently proposed by [Della Corte, Ramadorai, and Sarno \(2016\)](#). At the end of each month t , we compute the volatility risk premium (vrp) for each currency, that is, the difference between expected realized volatility and implied volatility over the next month.¹³ We sort all currencies available at time t into five quintile portfolios on the basis of their monthly vrp. The first quintile portfolio \mathcal{P}_1 comprises 20% of all currencies with the highest vrp, whereas the fifth quintile portfolio \mathcal{P}_5 contains 20% of all currencies with the lowest vrp. The difference between \mathcal{P}_1 and \mathcal{P}_5 is called the volatility risk premia strategy, which is equivalent to selling high insurance-cost currencies and buying low insurance-cost currencies.

3.8 Momentum Portfolios

We form an tradable strategy linked to the past performance of currencies as initially proposed by [Menkhoff, Sarno, Schmeling, and Schrimpf \(2012b\)](#). Recently, [Dahlquist and Hasseltoft \(2020\)](#) further connect currency returns to past trends in fundamentals including economic activity and inflation. At the end of each month t , we compute the average of currency excess returns over the last six months.¹⁴ We sort all currencies available at time t into five quintile portfolios on the basis of their trend. The first quintile portfolio \mathcal{P}_1 comprises 20% of all currencies with the highest average returns, whereas the fifth quintile portfolio \mathcal{P}_5 contains 20% of all currencies with the lowest average returns. The difference between \mathcal{P}_1 and \mathcal{P}_5 is called the momentum strategy (mom), which is equivalent to selling past losers (or worst performing currencies) and buying past winners (or best performing currencies).

4 Uncertainty Network Risk and Currency Returns

4.1 Net-directional Connectmonotonicityedness

Table 1 reports summary statistics of the excess returns of the five quintile portfolios ($\mathcal{P}_i : i = 1, \dots, 5$) and the long-short investment strategy buying \mathcal{P}_5 and selling \mathcal{P}_1 . Fur-

¹³[Della Corte, Ramadorai, and Sarno \(2016\)](#) work with the one-year volatility risk premium. We decide to switch to the monthly horizon to ensure that the volatility risk premium strategy employs one-month implied volatilities on exchange rates consistent with network connectedness portfolios.

¹⁴Our results remain quantitatively similar for other lags over which the past performance is evaluated.

ther, Panels A and B present the results for a horizon specific net-directional connectedness extracted from total and causal connections. Several observations from Table 1 are noteworthy.

First, the average returns of $\mathcal{N}(\mathcal{S})$ portfolios are 5.53% and 6.43% per annum for total and causal linkages, which are statistically different from zero at the 5% and 1% levels, respectively. The “fx (%)” and “ir (%)” rows further indicate that this predictability of the cross-sectional network strategy based on total connections is partially driven by predicting the interest rate differential. This result is expected in light of the prior literature (Menkhoff, Sarno, Schmeling, and Schrimpf, 2012a) documenting a link between global foreign exchange volatility, which is strongly reflected in contemporaneous covariances of network connectedness, and the carry trade strategy, which is entirely driven by the forward premium across countries. In contrast, the spread between \mathcal{P}_5 and \mathcal{P}_1 portfolios, which are constructed from the causal nature of network linkages, is largely driven by predicting the spot exchange rates. For instance, Panel B shows that the spread in the exchange rate component of the excess returns of $\mathcal{N}(\mathcal{S})$ is almost twice-as-large compared to the one reported in Panel A (4.33% versus 2.28% per annum), whereas the spread in the interest rate differential substantially shrinks (from 3.24% to 2.10% per annum). Also, the monotonicity in the forward premium does not hold as we move from \mathcal{P}_1 to \mathcal{P}_5 portfolios.

Second, the risk-adjusted performance of long-short portfolios deteriorates with the horizon of net-directional network risk. Using total network connectedness, the annualized Sharpe ratio of our network strategies gradually declines from 0.65 to 0.50 and 0.32 when using medium- and long- instead of short-term connections. The causal network zero-cost portfolios experience a steeper decline in the annualized Sharpe ratio from 0.80 to 0.47 and 0.39 when moving from short- to medium- and long-term horizons. Interestingly, the $\mathcal{N}(\mathcal{T})$ portfolio based on causal linkages exhibits the annualized Sharpe ratio of 0.66 and the average return of 4.90% per annum, which is statistically different from zero at 1% level. Overall, the performance of horizon specific network portfolios indicates the downward-sloping term structure of uncertainty network risk in the cross-section of exchange rates. This finding extends the results of the existing literature on the price of uncertainty risk in equity markets (Dew-Becker, Giglio, Le, and Rodriguez, 2017).

Table 1. Net-directional Network Portfolios

This table presents descriptive statistics for quintile ($\mathcal{P}_i : i = 1, \dots, 5$) and long-short portfolios ($\mathcal{N}(\cdot)$) sorted by short- (\mathcal{S}), medium- (\mathcal{M}), and long-term (\mathcal{L}) as well as total (\mathcal{T}) net-directional connectedness extracted from total (Panel A) and causal (Panel B) linkages. The portfolio $\mathcal{P}_1(\mathcal{P}_5)$ comprises currencies with the highest (lowest) network characteristic. The long-short portfolio buys \mathcal{P}_5 and sells \mathcal{P}_1 . Mean, standard deviation, and Sharpe ratio are annualized, but t-statistic of mean, skewness, kurtosis and the first-order autocorrelation are based on monthly returns. We also report the annualized mean of the exchange rate ($fx = -\Delta s^k$) and interest rate ($ir = i^k - i$) components of excess returns. The t-statistics are based on [Newey and West \(1987\)](#) standard errors with [Andrews \(1991\)](#) optimal lag selection. The sample is from January 1996 to December 2013.

Panel A: Total linkages												
	\mathcal{P}_1	\mathcal{P}_2	\mathcal{P}_3	\mathcal{P}_4	\mathcal{P}_5	$\mathcal{N}(\mathcal{S})$	\mathcal{P}_1	\mathcal{P}_2	\mathcal{P}_3	\mathcal{P}_4	\mathcal{P}_5	$\mathcal{N}(\mathcal{M})$
mean (%)	-0.69	0.35	1.65	1.44	4.84	5.53	-0.78	1.67	2.09	1.35	3.38	4.16
t-stat	-0.26	0.13	0.70	0.65	2.27	2.46	-0.30	0.63	0.87	0.68	1.34	1.83
fx (%)	-1.03	-0.45	-0.37	-1.30	1.26	2.28	-0.97	0.94	0.46	-1.44	-0.72	0.24
ir (%)	0.34	0.81	2.03	2.75	3.58	3.24	0.18	0.73	1.63	2.79	4.10	3.92
net	0.13	0.08	0.01	-0.06	-0.14	-0.27	0.07	0.05	0.00	-0.04	-0.08	-0.15
Sharpe	-0.06	0.03	0.18	0.16	0.61	0.65	-0.08	0.16	0.22	0.16	0.39	0.50
std (%)	10.70	10.48	9.36	8.80	7.91	8.52	10.35	10.30	9.34	8.70	8.76	8.29
skew	-0.15	-0.91	-0.48	-0.29	-0.13	-0.39	-0.22	-0.79	-0.13	-0.34	-1.34	-0.40
kurt	3.95	6.43	5.48	4.69	4.17	4.26	3.61	5.86	4.68	4.01	8.84	4.58
ac1	0.06	0.08	0.05	-0.04	0.13	0.10	0.02	0.05	0.06	-0.06	0.26	0.20
	\mathcal{P}_1	\mathcal{P}_2	\mathcal{P}_3	\mathcal{P}_4	\mathcal{P}_5	$\mathcal{N}(\mathcal{L})$	\mathcal{P}_1	\mathcal{P}_2	\mathcal{P}_3	\mathcal{P}_4	\mathcal{P}_5	$\mathcal{N}(\mathcal{T})$
mean (%)	0.05	0.41	2.54	1.94	2.81	2.76	-0.40	0.61	2.12	0.99	3.94	4.34
t-stat	0.02	0.15	1.01	0.85	1.33	1.20	-0.15	0.23	0.88	0.43	1.84	1.91
fx (%)	-0.16	-0.31	0.72	-0.79	-1.15	-0.99	-0.63	-0.03	0.28	-1.66	-0.10	0.53
ir (%)	0.22	0.72	1.82	2.73	3.96	3.74	0.23	0.64	1.84	2.65	4.04	3.81
net	0.05	0.03	0.00	-0.02	-0.05	-0.10	0.25	0.15	0.00	-0.13	-0.26	-0.52
Sharpe	0.01	0.04	0.26	0.22	0.33	0.32	-0.04	0.06	0.23	0.11	0.50	0.51
std (%)	10.51	9.83	9.86	8.72	8.42	8.70	10.68	10.06	9.16	9.40	7.81	8.43
skew	-0.46	-0.66	-0.15	-0.59	-0.65	0.01	-0.41	-0.48	-0.66	-0.45	-0.54	-0.29
kurt	4.77	5.15	4.87	6.21	4.82	5.12	4.95	4.23	5.67	4.46	4.01	4.13
ac1	0.04	0.13	0.03	0.03	0.08	0.09	0.04	0.07	0.04	0.02	0.16	0.12
Panel B: Causal linkages												
	\mathcal{P}_1	\mathcal{P}_2	\mathcal{P}_3	\mathcal{P}_4	\mathcal{P}_5	$\mathcal{N}(\mathcal{S})$	\mathcal{P}_1	\mathcal{P}_2	\mathcal{P}_3	\mathcal{P}_4	\mathcal{P}_5	$\mathcal{N}(\mathcal{M})$
mean (%)	-0.12	0.76	1.12	-0.18	6.31	6.43	-0.46	3.17	1.20	1.26	2.95	3.42
t-stat	-0.05	0.28	0.47	-0.07	3.11	3.81	-0.20	1.36	0.52	0.53	1.22	2.10
fx (%)	-2.14	-0.09	0.27	-1.68	2.20	4.33	-2.49	2.18	-0.27	-0.58	-0.10	2.39
ir (%)	2.01	0.84	0.84	1.50	4.11	2.10	2.03	0.99	1.47	1.84	3.05	1.02
net	0.03	0.00	-0.01	-0.01	-0.02	-0.05	0.03	-0.01	-0.01	-0.02	-0.03	-0.06
Sharpe	-0.01	0.08	0.12	-0.02	0.82	0.80	-0.05	0.36	0.13	0.13	0.32	0.47
std (%)	9.88	9.91	9.36	9.55	7.73	8.08	9.40	8.91	9.21	9.33	9.34	7.21
skew	-0.72	-0.90	-0.59	-0.22	-0.50	0.95	-0.87	-0.07	-0.54	-0.47	-0.63	0.07
kurt	5.32	5.62	5.63	4.72	4.07	6.86	5.79	3.68	4.43	4.99	5.61	3.46
ac1	-0.04	0.08	0.06	0.07	0.08	-0.15	0.01	0.05	0.02	0.06	0.10	-0.04
	\mathcal{P}_1	\mathcal{P}_2	\mathcal{P}_3	\mathcal{P}_4	\mathcal{P}_5	$\mathcal{N}(\mathcal{L})$	\mathcal{P}_1	\mathcal{P}_2	\mathcal{P}_3	\mathcal{P}_4	\mathcal{P}_5	$\mathcal{N}(\mathcal{T})$
mean (%)	-0.20	3.36	1.33	0.96	2.53	2.73	-0.26	2.11	1.04	0.33	4.64	4.90
t-stat	-0.09	1.36	0.55	0.41	1.05	1.83	-0.11	0.88	0.41	0.13	2.14	3.03
fx (%)	-2.20	1.98	-0.19	-0.69	-0.40	1.81	-2.27	1.26	-0.29	-1.33	1.12	3.39
ir (%)	2.00	1.38	1.52	1.65	2.92	0.93	2.01	0.84	1.33	1.65	3.52	1.51
net	0.03	0.00	-0.01	-0.02	-0.03	-0.06	0.10	-0.02	-0.04	-0.05	-0.08	-0.18
Sharpe	-0.02	0.36	0.14	0.11	0.26	0.39	-0.03	0.23	0.11	0.03	0.52	0.66
std (%)	9.16	9.36	9.50	8.88	9.64	7.07	9.47	9.08	9.67	9.44	8.89	7.44
skew	-0.77	-0.28	-0.43	-0.68	-0.50	0.01	-0.69	-0.27	-0.68	-0.36	-0.76	-0.32
kurt	5.56	3.51	4.07	5.30	5.27	3.47	5.17	3.77	5.27	4.66	5.89	4.94
ac1	0.00	0.05	0.04	0.09	0.05	-0.05	-0.02	0.03	0.04	0.16	0.05	-0.03

Table 2. To- and From-directional Network Portfolios: Causal Linkages

This table presents descriptive statistics for quintile ($\mathcal{P}_i : i = 1, \dots, 5$) and long-short portfolios ($\mathcal{T}(\cdot)$ and $\mathcal{F}(\cdot)$) sorted by short- (\mathcal{S}), medium- (\mathcal{M}), and long-term (\mathcal{L}) as well as total (\mathcal{T}) to-directional (Panel A) and from-directional (Panel B) connectedness extracted from causal linkages. The portfolio $\mathcal{P}_1(\mathcal{P}_5)$ comprises currencies with the highest (lowest) network characteristic. The long-short portfolio buys \mathcal{P}_5 and sells \mathcal{P}_1 . Mean, standard deviation, and Sharpe ratio are annualized, but t-statistic of mean, skewness, kurtosis and the first-order autocorrelation are based on monthly returns. We also report the average network characteristic (net), the annualized mean of the exchange rate ($fx = -\Delta s^k$) and interest rate ($ir = i^k - i$) components of excess returns. The t-statistics are based on [Newey and West \(1987\)](#) standard errors with [Andrews \(1991\)](#) optimal lag selection. The sample is from January 1996 to December 2013.

Panel A: To-directional network portfolios												
	\mathcal{P}_1	\mathcal{P}_2	\mathcal{P}_3	\mathcal{P}_4	\mathcal{P}_5	$\mathcal{T}(\mathcal{S})$	\mathcal{P}_1	\mathcal{P}_2	\mathcal{P}_3	\mathcal{P}_4	\mathcal{P}_5	$\mathcal{T}(\mathcal{M})$
mean (%)	0.04	0.00	-0.04	1.47	6.14	6.10	-0.61	0.92	0.16	1.54	5.91	6.52
t-stat	0.02	0.00	-0.02	0.66	3.13	3.66	-0.26	0.34	0.06	0.70	2.88	3.67
fx (%)	-1.92	-0.78	-0.89	-0.22	2.10	4.01	-2.52	-0.08	-0.63	-0.06	1.85	4.37
ir (%)	1.96	0.79	0.85	1.68	4.05	2.09	1.91	0.99	0.79	1.60	4.06	2.15
net	1.13	1.05	1.04	1.03	1.01	-0.12	1.37	1.18	1.13	1.09	1.05	-0.31
Sharpe	0.00	0.00	0.00	0.16	0.82	0.74	-0.06	0.09	0.02	0.18	0.77	0.80
std (%)	9.79	10.11	10.32	8.88	7.47	8.27	9.96	10.24	9.71	8.76	7.64	8.13
skew	-0.53	-0.83	-0.80	-0.47	-0.46	0.36	-0.61	-0.80	-0.71	-0.20	-0.40	0.24
kurt	4.45	6.26	5.75	4.94	4.15	5.30	4.40	5.78	5.78	4.09	4.01	4.00
ac1	-0.08	0.12	0.07	0.07	0.05	-0.15	-0.05	0.09	0.02	0.08	0.09	-0.11
	\mathcal{P}_1	\mathcal{P}_2	\mathcal{P}_3	\mathcal{P}_4	\mathcal{P}_5	$\mathcal{T}(\mathcal{L})$	\mathcal{P}_1	\mathcal{P}_2	\mathcal{P}_3	\mathcal{P}_4	\mathcal{P}_5	$\mathcal{T}(\mathcal{T})$
mean (%)	-0.48	0.64	0.38	1.25	6.13	6.61	-0.36	0.38	1.01	1.15	5.63	5.99
t-stat	-0.20	0.25	0.15	0.55	2.96	3.99	-0.15	0.14	0.39	0.55	2.74	3.49
fx (%)	-2.37	-0.18	-0.61	-0.25	1.97	4.35	-2.32	-0.59	0.20	-0.38	1.57	3.89
ir (%)	1.89	0.82	0.99	1.50	4.16	2.26	1.96	0.97	0.81	1.53	4.06	2.10
net	1.60	1.32	1.25	1.18	1.11	-0.49	1.27	1.12	1.09	1.06	1.03	-0.24
Sharpe	-0.05	0.06	0.04	0.14	0.80	0.83	-0.04	0.04	0.10	0.13	0.73	0.74
std (%)	9.65	10.27	9.83	9.06	7.69	7.99	10.02	9.98	9.94	8.66	7.66	8.05
skew	-0.48	-0.53	-0.56	-0.64	-0.41	0.26	-0.74	-0.63	-0.93	-0.26	-0.39	0.33
kurt	3.99	4.24	5.62	5.12	4.03	4.09	5.08	5.10	6.47	4.33	4.01	4.29
ac1	-0.02	0.04	0.01	0.10	0.07	-0.19	-0.05	0.10	0.05	0.04	0.09	-0.13
Panel B: From-directional network portfolios												
	\mathcal{P}_1	\mathcal{P}_2	\mathcal{P}_3	\mathcal{P}_4	\mathcal{P}_5	$\mathcal{F}(\mathcal{S})$	\mathcal{P}_1	\mathcal{P}_2	\mathcal{P}_3	\mathcal{P}_4	\mathcal{P}_5	$\mathcal{F}(\mathcal{M})$
mean (%)	0.85	1.97	1.85	1.49	1.51	0.67	0.57	1.47	1.86	2.41	1.98	1.41
t-stat	0.33	0.75	0.77	0.71	0.72	0.43	0.21	0.56	0.86	1.13	0.92	0.85
fx (%)	-1.51	0.25	0.29	-0.26	-0.62	0.89	-1.19	0.22	0.19	0.44	-0.86	0.33
ir (%)	2.36	1.72	1.56	1.75	2.14	-0.22	1.76	1.25	1.67	1.97	2.84	1.08
net	1.07	1.06	1.05	1.05	1.05	-0.02	1.39	1.29	1.24	1.19	1.13	-0.26
Sharpe	0.08	0.21	0.19	0.17	0.18	0.09	0.05	0.15	0.21	0.27	0.25	0.19
std (%)	10.76	9.54	9.51	8.68	8.30	7.26	10.68	9.85	9.04	8.88	7.96	7.58
skew	-0.50	-0.87	-0.46	0.02	-0.64	0.02	-0.59	-0.73	-0.28	-0.69	-0.11	-0.03
kurt	4.23	5.24	5.73	3.30	4.78	3.63	4.99	5.23	4.12	5.07	3.31	3.90
ac1	-0.01	0.20	0.02	-0.04	0.06	-0.11	0.04	0.09	0.06	0.01	0.07	-0.03
	\mathcal{P}_1	\mathcal{P}_2	\mathcal{P}_3	\mathcal{P}_4	\mathcal{P}_5	$\mathcal{F}(\mathcal{L})$	\mathcal{P}_1	\mathcal{P}_2	\mathcal{P}_3	\mathcal{P}_4	\mathcal{P}_5	$\mathcal{F}(\mathcal{T})$
mean (%)	1.48	1.19	0.98	2.46	2.07	0.59	-0.37	2.93	2.42	1.11	2.15	2.52
t-stat	0.58	0.46	0.40	1.11	0.98	0.36	-0.14	1.15	1.14	0.49	1.00	1.59
fx (%)	-0.29	-0.04	-0.62	0.41	-0.77	-0.48	-2.28	1.58	0.69	-0.92	-0.36	1.92
ir (%)	1.77	1.22	1.60	2.05	2.84	1.07	1.91	1.35	1.74	2.04	2.51	0.60
net	2.05	1.74	1.57	1.41	1.23	-0.83	1.24	1.19	1.16	1.13	1.09	-0.15
Sharpe	0.15	0.12	0.11	0.27	0.25	0.08	-0.04	0.29	0.28	0.12	0.27	0.34
std (%)	10.11	9.97	9.25	9.11	8.36	7.22	10.54	10.24	8.67	9.09	8.02	7.40
skew	-0.38	-0.58	-0.87	0.03	-0.30	0.01	-0.44	-0.92	-0.30	-0.56	-0.20	-0.31
kurt	4.37	5.19	6.00	4.24	4.42	3.20	4.54	6.21	4.79	4.53	3.20	4.26
ac1	0.04	0.07	0.09	0.03	0.02	-0.06	0.02	0.04	0.04	0.03	0.08	-0.04

Third, the excess returns of the best-performing network portfolio based on causal short-term linkages exhibit a low standard deviation, a positive skew and a sizeable kurtosis. The volatility statistic implies that the improved Sharpe ratio originates not only from higher returns but also from their moderate time-variation. According to the skewness and kurtosis statistics, the portfolio is the only one among other specifications that tends to experience gains rather than losses, with more outliers in the right tail of the distribution. Indeed, analyzing the strategy's best and worst months, the portfolio experiences the three highest monthly returns of 7.98% in September 2002, 8.49% in August 1998, and 13.07% in October 2008, and the three lowest monthly returns of -4.61% in July 2002, -4.66% in August 2002, and -4.85% in January 1998. In contrast, the excess returns of the network portfolio based on total short-term linkages has a negative skewness, reflecting smaller maximal growth rates (6.10% in February 1997, 6.23% in October 1998, and 7.17% in May 2005) and deeper crashes (-6.18% in June 2002, -6.20% in December 2000, and -10.02% in December 2008).

4.2 *To- and From-directional Connectedness*

Table 2 presents the performance statistics of the excess returns sorted on to-directional (Panel A) and from-directional (Panel B) connectedness extracted from causal linkages. The table shows the results for horizon-specific network risk measures.

For the to-directional case, the spread between the excess returns of \mathcal{P}_5 and \mathcal{P}_1 portfolios is increasing in the horizon and is statistically significant at the 1% level for all cases. Also, one can generally observe a monotonic pattern in the average excess returns of quintile portfolios, particularly for the cases of longer-term and total-horizon network risks. Consequently, the long-short currency portfolios based on the amount of transmitted shocks have the annualized Sharpe ratios ranging from 0.74 to 0.83 for the short- and long-term horizon connectedness. All zero-cost investment strategies display a positive skew of their excess returns. Interestingly, this performance primarily stems from the exchange rate predictability, while the interest rate differential contributes less. For the from-directional case, the results indicate no clear patterns in the performance statistics of currency network strategies taking into account the information about the received shocks. Although the average excess returns of quintile and long-short portfolios tend to be positive, they remain insignificant at all conventional confidence levels. This ultimately leads to much

smaller Sharpe ratios compared to those from other strategies.

Overall, the results presented in Table 2 suggest that the impact of a particular currency on exchange rates of other countries is the key to understanding the profitability of net-directional network portfolios. Specifically, we document that the currencies transmitting more shocks to others (in the net or total amount) tend to appreciate, leading to lower currency risk premia. Unlike the carry trade strategy, we demonstrate that the stronger transmitters of causal shocks do not necessarily have the lowest interest rates. By connecting currency returns to uncertainty network risk extracted from currency option data, we shed light on the novel risk that drives international asset prices above and beyond the existing risks capturing macroeconomic country-specific conditions and trade connections among others.

4.3 Relationship with Benchmark Strategies and Diversification Gains

We now study the relationship between the network long-short portfolios and existing benchmarks. We begin by reporting the summary statistics of the standard dollar, carry trade, volatility, variance risk premium, and momentum strategies as well as an equally weighted average of all currency benchmarks in Table 3. The carry and momentum strategies exhibit the highest Sharpe ratios of 0.69 and 0.38, with the former having a statistically significant mean excess return. However, both have a negative skewness, indicating the possibility of large losses. The last column shows limited diversification gains from equally combining all strategies as indicated by a tiny increase in the Sharpe ratio and a negative skewness of the “1/N” portfolio.

Next we examine how well the benchmark strategies can explain the network portfolios. We perform a two-step analysis. First, we compute the sample correlations between the excess returns of different strategies. Second, for the zero-cost network portfolios, we run contemporaneous regressions using their monthly returns as dependent variables and benchmark strategies as independent variables. Tables 4 and 5 report the results of the two-stage procedure for investment strategies constructed in Sections 4.1 and 4.2.

Several observations in Table 4 are worth discussing. First, the currency portfolio returns sorted on total network connectedness tend to be more correlated with benchmark strategies than those based on causal linkages. Also, the negative correlations of total

Table 3. Benchmark Strategies: Summary Statistics

This table presents descriptive statistics (Panel A) and correlations (Panel B) between dollar (dol), carry trade (car), volatility (vol), volatility risk premium (vrp), momentum (mom) strategies and an equally weighted average of all currency benchmarks (1/N). Mean, standard deviation, and Sharpe ratio are annualized, but t-statistic of mean, skewness, kurtosis and the first-order autocorrelation are based on monthly returns. The t-statistics are based on [Newey and West \(1987\)](#) standard errors with [Andrews \(1991\)](#) optimal lag selection. The sample is from January 1996 to December 2013.

Panel A: Benchmark strategies						
	dol	car	vol	vrp	mom	1/N
mean (%)	1.60	7.29	2.28	1.66	3.64	3.30
t-stat	0.75	2.58	1.04	0.84	1.66	2.55
Sharpe	0.20	0.69	0.25	0.21	0.38	0.71
std (%)	8.16	10.52	8.98	8.04	9.49	4.62
skew	-0.60	-0.68	0.12	0.04	-0.17	-0.69
kurt	5.19	4.48	3.36	3.46	3.02	6.24
ac1	0.07	0.12	0.06	0.11	-0.04	0.14
Panel B: Correlations						
	dol	car	vol	vrp	mom	1/N
dol	1.00	0.33	0.61	-0.07	0.01	0.72
car	0.33	1.00	0.28	-0.29	0.23	0.68
vol	0.61	0.28	1.00	-0.17	-0.20	0.58
vrp	-0.07	-0.29	-0.17	1.00	-0.05	0.10
mom	0.01	0.23	-0.20	-0.05	1.00	0.42
1/N	0.72	0.68	0.58	0.10	0.42	1.00

(causal) connectedness portfolios with vol and vrp (car and vol) provide the scope for diversification benefits. Second, the strength of the correlations directly translates into the significant coefficients for car, vol and vrp (Panel B for total linkages). We can conclude that the significant portion of the excess returns obtained from total connectedness measures reflects interest rate differentials and global components of realized and implied currency variances. Third, once the contemporaneous effects are removed, none of the four factors appear to be significant (the right part of Panel B). Also, the predictive power of the four benchmarks for network portfolios dramatically drops as measured by the adjusted R^2 , which range from 9.36% to 31.05% for total linkages and are around 2% for causal linkages. Fourth, the resulting alphas for $\mathcal{N}(\mathcal{S})$ are economically and statistically significant for both network risk measures. For instance, the annualized alphas of 5.00% and 6.58% are close to the average returns of 5.53% and 6.43% for the corresponding $\mathcal{N}(\mathcal{S})$ strategies, that is, less than 10% of the network returns are explained by the four benchmark strategies. Panel C in Table 4 shows that the inclusion of the dollar slightly reduces the estimated alphas and increases the adjusted R^2 statistics, but the significance of constants

remains unchanged.

Table 5 replicates the analysis separately for the currency returns sorted on to-directional and from-directional causal connections. It demonstrates that the transmitted shocks in the global network of currencies play the key role. Indeed, all $\mathcal{T}(\mathcal{H}) : \mathcal{H} \in \{\mathcal{S}, \mathcal{M}, \mathcal{L}, \mathcal{T}\}$ generate highly significant performance, both economically and statistically, which cannot be understood through the lens of the benchmarks.

We further investigate the diversification benefits of our network portfolios. For the ease of the presentation, we focus on short-term net-directional network cases (both total and causal). We implement a naive strategy combining the network portfolio and one of the benchmarks with 0.5-0.5 weights. Table 6 report the results. For the strategies based on total connectedness, the resulting Sharpe ratios become considerably higher relative to the individual benchmarks, with the increase ranging from 26% for car and to well above 200% for dol and vrp. As can be expected from the correlation analysis, the causal connectedness portfolio leads to larger levels and differences in Sharpe ratios. For instance, the allocation in $\mathcal{N}(\mathcal{S})$ and car generates the ratios of 1.08, which is 56.52% higher than the original carry trade.

Finally, we now provide the allocation analysis of selected portfolios: $\mathcal{N}(\mathcal{S})$ (causal linkages), car, vol, vrp, and mom. Table 7 reports the fraction of months each investment strategy goes long (the “Buy” columns) or short (the “Sell” columns) in each currency. We also compute the fraction of months when the currency position in $\mathcal{N}(\mathcal{S})$ is different from the currency allocation in the benchmarks (the “Diff” columns). The bottom row shows the average fraction of “Diff” statistics across the currencies.

Table 7 demonstrates significant differences across strategies and countries. For instance, the network strategy on average buys or sells alternative currencies in 40%, 46%, 47%, and 44% of the time relative to the carry, volatility, variance risk premium, and momentum strategies. The countries whose allocations differ most in their distributions relative to $\mathcal{N}(\mathcal{S})$ are Japan and Switzerland for the carry trade, South Africa and Mexico for volatility, Mexico and South Africa for variance risk premium, Japan and South Africa for momentum. Most notably, if we sort the currencies according to interest rate differentials, we would have bought South African rand (ZAR) in 92% of months and would have al-

Table 4. Net-directional Network Portfolios and Benchmark Strategies

This table presents correlations (Panel A) and a contemporaneous regression (Panels B and C) of the monthly returns of net-directional network portfolios ($\mathcal{N}(\mathcal{H}) : \mathcal{H} \in \{\mathcal{S}, \mathcal{M}, \mathcal{L}, \mathcal{T}\}$) on benchmark strategies - dollar (dol), carry trade (car), volatility (vol), volatility risk premium (vrp), and momentum (mom). Constants reported in the “alpha (% annual)” row are expressed in percentage per annum. The numbers in rows with a grey font are t-statistics of the estimates. The t-statistics are based on [Newey and West \(1987\)](#) standard errors with [Andrews \(1991\)](#) optimal lag selection. The last two rows report adjusted R^2 values (in percentage) and the number of observations. The sample is from January 1996 to December 2013.

Panel A: Correlations with trading strategies								
	Total linkages				Causal linkages			
	$\mathcal{N}(\mathcal{S})$	$\mathcal{N}(\mathcal{M})$	$\mathcal{N}(\mathcal{L})$	$\mathcal{N}(\mathcal{T})$	$\mathcal{N}(\mathcal{S})$	$\mathcal{N}(\mathcal{M})$	$\mathcal{N}(\mathcal{L})$	$\mathcal{N}(\mathcal{T})$
dol	-0.41	-0.25	-0.32	-0.41	-0.24	0.02	0.11	-0.05
car	0.20	0.46	0.36	0.29	-0.09	0.01	0.00	0.04
vol	-0.14	-0.13	-0.11	-0.20	-0.15	-0.12	-0.09	-0.12
vrp	-0.19	-0.29	-0.22	-0.26	0.09	0.04	0.08	-0.01
mom	0.14	0.21	0.12	0.18	0.11	0.17	0.18	0.20
Panel B: Returns of network portfolios on benchmark strategies (without dollar)								
	Total linkages				Causal linkages			
	$\mathcal{N}(\mathcal{S})$	$\mathcal{N}(\mathcal{M})$	$\mathcal{N}(\mathcal{L})$	$\mathcal{N}(\mathcal{T})$	$\mathcal{N}(\mathcal{S})$	$\mathcal{N}(\mathcal{M})$	$\mathcal{N}(\mathcal{L})$	$\mathcal{N}(\mathcal{T})$
alpha (% annual)	5.00	2.28	1.37	3.53	6.58	3.06	2.28	4.46
	2.29	1.18	0.55	1.66	3.35	1.63	1.32	2.39
car	0.16	0.38	0.32	0.24	-0.05	0.00	-0.01	0.01
	1.71	6.22	2.81	2.60	-0.60	0.04	-0.16	0.24
vol	-0.21	-0.27	-0.25	-0.29	-0.09	-0.06	-0.03	-0.07
	-2.07	-3.83	-3.97	-4.00	-1.51	-1.19	-0.51	-1.35
vrp	-0.18	-0.21	-0.17	-0.23	0.06	0.03	0.07	-0.01
	-2.22	-2.42	-1.95	-2.67	0.69	0.45	1.05	-0.08
mom	0.04	0.02	-0.03	0.03	0.10	0.12	0.13	0.14
	0.48	0.36	-0.33	0.47	1.25	1.67	1.90	1.97
$R^2(\%)$	9.36	31.05	18.40	19.70	2.17	1.95	2.22	2.90
Number of obs.	215	215	215	215	215	215	215	215
Panel C: Returns of network portfolios on benchmark strategies (with dollar)								
	Total linkages				Causal linkages			
	$\mathcal{N}(\mathcal{S})$	$\mathcal{N}(\mathcal{M})$	$\mathcal{N}(\mathcal{L})$	$\mathcal{N}(\mathcal{T})$	$\mathcal{N}(\mathcal{S})$	$\mathcal{N}(\mathcal{M})$	$\mathcal{N}(\mathcal{L})$	$\mathcal{N}(\mathcal{T})$
alpha (% annual)	4.36	1.83	0.80	2.92	6.31	3.17	2.48	4.44
	2.14	0.92	0.36	1.54	3.48	1.66	1.39	2.40
dol	-0.62	-0.44	-0.55	-0.59	-0.26	0.11	0.20	-0.01
	-7.43	-5.25	-5.64	-6.92	-2.70	1.37	2.52	-0.16
car	0.24	0.44	0.39	0.32	-0.02	-0.01	-0.04	0.02
	3.47	7.34	4.50	5.00	-0.26	-0.19	-0.59	0.26
vol	0.12	-0.03	0.05	0.02	0.05	-0.12	-0.14	-0.07
	1.21	-0.40	0.64	0.32	0.61	-1.94	-2.05	-1.06
vrp	-0.13	-0.17	-0.12	-0.18	0.08	0.02	0.05	0.00
	-1.78	-2.24	-1.55	-2.40	0.99	0.29	0.75	-0.06
mom	0.09	0.06	0.02	0.08	0.12	0.11	0.12	0.14
	1.46	1.14	0.21	1.53	1.46	1.60	1.81	1.98
$R^2(\%)$	30.21	41.84	34.11	38.97	5.89	2.38	4.97	2.45
Number of obs.	215	215	215	215	215	215	215	215

Table 5. To- and From-directional Network Portfolios and Benchmark Strategies

This table presents correlations (Panel A) and a contemporaneous regression (Panels B and C) of the monthly returns of to- and from-directional network portfolios ($\mathcal{T}(\mathcal{H})$ and $\mathcal{F}(\mathcal{H}) : \mathcal{H} \in \{\mathcal{S}, \mathcal{M}, \mathcal{L}, \mathcal{T}\}$) on benchmark strategies - dollar (dol), carry trade (car), volatility (vol), volatility risk premium (vRP), and momentum (mom). Constants reported in the “alpha (%, annual)” row are expressed in percentage per annum. The numbers in rows with a grey font are t-statistics of the estimates. The t-statistics are based on [Newey and West \(1987\)](#) standard errors with [Andrews \(1991\)](#) optimal lag selection. The last two rows report adjusted R^2 values (in percentage) and the number of observations. The sample is from January 1996 to December 2013.

Panel A: Correlations with trading strategies

	Causal linkages							
	$\mathcal{T}(\mathcal{S})$	$\mathcal{T}(\mathcal{M})$	$\mathcal{T}(\mathcal{L})$	$\mathcal{T}(\mathcal{T})$	$\mathcal{F}(\mathcal{L})$	$\mathcal{F}(\mathcal{M})$	$\mathcal{F}(\mathcal{L})$	$\mathcal{F}(\mathcal{T})$
dol	-0.27	-0.27	-0.20	-0.26	-0.35	-0.42	-0.27	-0.38
car	-0.09	-0.04	-0.03	-0.07	-0.08	-0.03	0.13	-0.05
vol	-0.14	-0.17	-0.19	-0.15	-0.14	-0.08	-0.12	-0.07
vRP	0.10	0.08	0.06	0.07	-0.03	-0.07	-0.09	-0.07
mom	0.14	0.16	0.14	0.14	-0.14	-0.09	-0.01	-0.11

Panel B: Returns of network portfolios on benchmark strategies (without dollar)

	Causal linkages							
	$\mathcal{T}(\mathcal{S})$	$\mathcal{T}(\mathcal{M})$	$\mathcal{T}(\mathcal{L})$	$\mathcal{T}(\mathcal{T})$	$\mathcal{F}(\mathcal{L})$	$\mathcal{F}(\mathcal{M})$	$\mathcal{F}(\mathcal{L})$	$\mathcal{F}(\mathcal{T})$
alpha (%, annual)	6.14	6.39	6.53	6.05	1.67	2.13	0.44	3.34
	3.20	3.15	3.52	3.07	1.03	1.20	0.27	1.99
car	-0.06	-0.02	0.00	-0.04	-0.01	0.00	0.13	-0.01
	-0.72	-0.24	-0.01	-0.51	-0.13	0.04	2.31	-0.19
vol	-0.07	-0.11	-0.14	-0.09	-0.15	-0.10	-0.17	-0.09
	-1.17	-1.67	-2.24	-1.42	-2.16	-1.12	-1.89	-1.08
vRP	0.07	0.06	0.04	0.04	-0.07	-0.09	-0.07	-0.09
	0.73	0.60	0.46	0.47	-1.05	-1.44	-1.11	-1.43
mom	0.13	0.12	0.09	0.11	-0.14	-0.10	-0.08	-0.10
	1.68	1.59	1.17	1.40	-2.72	-1.65	-1.29	-1.94
$R^2(%)$	2.81	2.93	3.12	2.23	3.57	0.85	3.97	1.08
Number of obs.	215	215	215	215	215	215	215	215

Panel C: Returns of network portfolios on benchmark strategies (with dollar)

	Causal linkages							
	$\mathcal{T}(\mathcal{S})$	$\mathcal{T}(\mathcal{M})$	$\mathcal{T}(\mathcal{L})$	$\mathcal{T}(\mathcal{T})$	$\mathcal{F}(\mathcal{L})$	$\mathcal{F}(\mathcal{M})$	$\mathcal{F}(\mathcal{L})$	$\mathcal{F}(\mathcal{T})$
alpha (%, annual)	5.81	6.07	6.36	5.74	1.29	1.54	0.12	2.84
	3.20	3.20	3.53	3.09	0.77	0.96	0.07	1.81
dol	-0.33	-0.31	-0.16	-0.30	-0.37	-0.57	-0.31	-0.49
	-3.04	-3.38	-1.63	-3.51	-5.75	-6.63	-3.59	-5.08
car	-0.02	0.02	0.02	-0.01	0.04	0.08	0.17	0.05
	-0.27	0.29	0.26	-0.07	0.78	1.56	3.14	1.06
vol	0.10	0.06	-0.05	0.07	0.05	0.20	0.00	0.17
	1.10	0.66	-0.61	0.85	0.67	2.20	-0.01	1.87
vRP	0.10	0.08	0.06	0.07	-0.03	-0.04	-0.04	-0.05
	1.11	0.96	0.61	0.80	-0.58	-0.78	-0.74	-0.92
mom	0.16	0.14	0.11	0.14	-0.11	-0.05	-0.05	-0.06
	1.96	1.84	1.30	1.66	-2.27	-1.05	-0.93	-1.30
$R^2(%)$	8.61	8.28	4.32	7.24	13.38	22.73	10.86	18.09
Number of obs.	215	215	215	215	215	215	215	215

Table 6. Benchmark Strategies: Diversification Gains

This table presents the impact of adding short-term net-directional strategy ($\mathcal{N}(\mathcal{S})$) to benchmark strategies - dollar (dol), carry trade (car), volatility (vol), volatility risk premium (vrp), and momentum (mom). We construct a naive 50%-50% portfolio of $\mathcal{N}(\mathcal{S})$ and one of benchmark strategies. The “1/N” column presents the statistics of an equally weighted portfolio of all benchmarks and a network strategy. Panel A (B) reports the results for the case of total (causal) linkages. Mean, standard deviation, and Sharpe ratio are annualized, but t-statistic of mean, skewness, kurtosis and the first-order autocorrelation are based on monthly returns. The t-statistics are based on [Newey and West \(1987\)](#) standard errors with [Andrews \(1991\)](#) optimal lag selection. The last row in each panel shows the percentage increase in the Sharpe ratio of a diversified portfolio relative to the original benchmark strategy. The sample is from January 1996 to December 2013.

Panel A: Including short-term net-directional strategy: total linkages						
	dol	car	vol	vrp	mom	1/N
	+ $\mathcal{N}(\mathcal{S})$					
mean (%)	3.56	6.41	3.91	3.59	4.58	4.41
t-stat	2.75	3.13	2.79	3.00	2.59	3.49
Sharpe	0.78	0.87	0.68	0.68	0.67	0.96
std (%)	4.55	7.39	5.72	5.26	6.80	4.60
skew	-0.17	-0.21	0.07	-0.22	-0.26	-0.20
kurt	3.67	3.41	5.83	4.00	3.27	4.17
ac1	0.13	0.15	0.00	0.00	0.02	0.09
% Δ Sharpe	290.00	26.09	172.00	223.81	76.32	35.21

Panel B: Including short-term net-directional strategy: causal linkages						
	dol	car	vol	vrp	mom	1/N
	+ $\mathcal{N}(\mathcal{S})$					
mean (%)	4.01	6.86	4.36	4.05	5.04	4.86
t-stat	3.24	4.13	3.07	3.21	3.76	4.73
Sharpe	0.80	1.08	0.78	0.68	0.77	1.10
std (%)	5.00	6.34	5.56	5.96	6.57	4.43
skew	-0.60	-0.28	0.11	0.34	0.14	-0.15
kurt	3.53	3.87	3.28	4.79	4.47	3.56
ac1	0.00	0.13	0.04	-0.03	-0.14	-0.03
% Δ Sharpe	300.00	56.52	212.00	223.81	102.63	54.93

ways kept Japanese yen (JPY) in the short position. In contrast, our causal net-directional connectedness strategy buys and sells JPY in 27% and 22% of the time and ZAR - 33% and 25%.

4.4 Daily and Weekly Frequencies

Given the availability of the daily network connectedness data, it is reasonable to ask whether the profits of network strategies are sensitive to the frequency of rebalancing. We therefore construct horizon specific net-directional network portfolios (total and causal linkages) and the benchmark strategies at the daily and weekly frequencies. Specifically, we

Table 7. Allocation Analysis for the Network Portfolio and Benchmark Strategies

This table presents an allocation analysis of a short-term net-directional network portfolio based on causal linkages ($\mathcal{N}(\mathcal{S})$) and carry trade (car), volatility (vol), volatility risk premium (vrp), and momentum (mom) strategies. The “Buy” and “Sell” columns report the fraction of months each currency belongs to the long and short positions of portfolios considered. The “Diff” column for each benchmark strategy reports the fraction of months the position for a particular currency is different from the one in $\mathcal{N}(\mathcal{S})$. The bottom row reports the average fraction across the currencies. The sample is from January 1996 to December 2013.

	$\mathcal{N}(\mathcal{S})$		car			vol			vrp			mom		
	Buy	Sell	Buy	Sell	Diff									
Australia	0.25	0.15	0.00	0.00	0.40	0.26	0.02	0.53	0.28	0.10	0.53	0.25	0.16	0.57
Brazil	0.41	0.06	0.67	0.00	0.26	0.23	0.07	0.47	0.12	0.36	0.53	0.35	0.10	0.38
Canada	0.10	0.25	0.00	0.07	0.37	0.02	0.54	0.60	0.24	0.08	0.47	0.17	0.20	0.52
Czech Republic	0.06	0.12	0.00	0.07	0.23	0.17	0.01	0.28	0.17	0.08	0.29	0.09	0.09	0.23
Denmark	0.00	0.15	0.00	0.10	0.20	0.05	0.07	0.25	0.07	0.08	0.28	0.09	0.16	0.33
Euro Area	0.01	0.17	0.00	0.26	0.24	0.05	0.06	0.27	0.09	0.08	0.30	0.06	0.15	0.25
Hungary	0.13	0.16	0.53	0.00	0.48	0.34	0.00	0.48	0.16	0.20	0.42	0.24	0.10	0.38
Japan	0.27	0.22	0.00	1.00	0.78	0.24	0.13	0.50	0.26	0.23	0.58	0.16	0.40	0.65
Mexico	0.59	0.12	0.36	0.00	0.59	0.09	0.36	0.71	0.11	0.40	0.67	0.27	0.25	0.56
New Zealand	0.13	0.20	0.24	0.00	0.38	0.40	0.02	0.55	0.34	0.18	0.54	0.27	0.14	0.51
Norway	0.04	0.20	0.08	0.00	0.29	0.19	0.04	0.40	0.23	0.13	0.51	0.13	0.12	0.40
Poland	0.27	0.09	0.18	0.00	0.34	0.40	0.03	0.52	0.21	0.24	0.55	0.26	0.11	0.40
Singapore	0.07	0.27	0.00	0.48	0.36	0.00	0.66	0.40	0.10	0.04	0.34	0.04	0.15	0.38
South Africa	0.33	0.25	0.92	0.00	0.64	0.59	0.14	0.80	0.21	0.52	0.67	0.31	0.27	0.60
South Korea	0.40	0.00	0.00	0.00	0.40	0.02	0.27	0.45	0.07	0.20	0.44	0.11	0.08	0.38
Sweden	0.06	0.16	0.00	0.12	0.28	0.19	0.02	0.34	0.23	0.12	0.47	0.10	0.16	0.40
Switzerland	0.06	0.30	0.00	0.98	0.69	0.19	0.03	0.49	0.27	0.10	0.59	0.14	0.25	0.53
Taiwan	0.09	0.35	0.00	0.41	0.33	0.00	0.71	0.37	0.10	0.09	0.43	0.05	0.27	0.43
Turkey	0.17	0.20	0.55	0.00	0.38	0.12	0.10	0.39	0.08	0.23	0.34	0.19	0.11	0.39
United Kingdom	0.11	0.14	0.01	0.06	0.32	0.01	0.27	0.33	0.21	0.09	0.39	0.18	0.16	0.48
Average					0.40			0.46			0.47			0.44

use the daily observations of currency connectedness from the core analysis and sample the daily or end-of-week observations to construct long-short portfolios. The realized volatility and variance risk premium are computed on the rolling one-month window, while the currency momentum is computed over the rolling six-month horizon. For daily and weekly frequencies, Tables 8 and 9 report summary statistics of the long-short portfolios (Panels A and B), regression outputs with the network excess returns as dependent variables and benchmarks as independent variables (Panel C).

Several interesting observations emerge from this investigation. First, the Sharpe ratios of short-term (long-term) network portfolios sorted on total connectedness decline (increase) with more frequent rebalancing, whereas the medium-term and total connections are priced similarly. Second, the Sharpe ratios of the causal network strategies for all horizons substantially increase for weekly and especially daily frequency: 0.99, 0.57, 0.57, 0.64 (weekly) and 1.13, 0.72, 0.71, 0.84 (daily) for $\mathcal{N}(\mathcal{H}) : \mathcal{H} \in \{\mathcal{S}, \mathcal{M}, \mathcal{L}, \mathcal{T}\}$, respectively. Thus, we similarly document the downward-sloping term structure of causal

Table 8. Daily Frequency

This table presents a robustness analysis of currency strategies implemented on a daily frequency. It reports descriptive statistics of net-directional network portfolios (Panel A) and benchmark strategies (Panel B), and a contemporaneous regression (Panel C) of the daily returns of net-directional network portfolios ($\mathcal{N}(\mathcal{H})$: $\mathcal{H} \in \{\mathcal{S}, \mathcal{M}, \mathcal{L}, \mathcal{T}\}$) on benchmark strategies - dollar (dol), carry trade (car), volatility (vol), volatility risk premium (vrp), and momentum (mom). In Panels A and B, mean, standard deviation, and Sharpe ratio are annualized, but t-statistic of mean, skewness, kurtosis and the first-order autocorrelation are based on daily returns. In Panel C, constants reported in the “alpha (%, annual)” row are expressed in percentage per annum. The numbers in rows with a grey font are t-statistics of the estimates. The t-statistics are based on [Newey and West \(1987\)](#) standard errors with [Andrews \(1991\)](#) optimal lag selection. The last two rows report adjusted R^2 values (in percentage) and the number of observations. The sample is from January 1996 to December 2013.

Panel A: Performance of network portfolios								
	Total linkages				Causal linkages			
	$\mathcal{N}(\mathcal{S})$	$\mathcal{N}(\mathcal{M})$	$\mathcal{N}(\mathcal{L})$	$\mathcal{N}(\mathcal{T})$	$\mathcal{N}(\mathcal{S})$	$\mathcal{N}(\mathcal{M})$	$\mathcal{N}(\mathcal{L})$	$\mathcal{N}(\mathcal{T})$
mean (%)	4.22	4.72	4.46	4.57	9.91	6.13	5.73	7.02
t-stat	2.04	2.34	2.10	2.14	4.96	3.14	3.02	3.65
Sharpe	0.47	0.50	0.47	0.47	1.13	0.72	0.71	0.84
std (%)	9.02	9.41	9.50	9.65	8.81	8.51	8.07	8.41
skew	-0.18	-0.08	0.17	0.38	0.36	0.39	0.36	0.06
kurt	5.52	7.19	11.59	11.96	17.92	15.28	8.70	14.76
ac1	-0.05	-0.05	-0.07	-0.09	-0.04	-0.03	0.01	-0.03
Panel B: Performance of benchmark strategies								
	dol					car	vol	vrp
	mean (%)	1.62	7.23	1.86	6.13	0.40		
t-stat	0.85	2.87	0.84	2.86	0.17			
Sharpe	0.21	0.65	0.18	0.65	0.04			
std (%)	7.64	11.14	10.47	9.38	10.49			
skew	-0.03	-0.67	-0.05	0.61	-0.48			
kurt	8.08	11.21	8.40	9.57	9.89			
ac1	0.04	-0.01	-0.04	-0.03	0.02			
Panel C: Returns of network portfolios on benchmark strategies								
	Total linkages				Causal linkages			
	$\mathcal{N}(\mathcal{S})$	$\mathcal{N}(\mathcal{M})$	$\mathcal{N}(\mathcal{L})$	$\mathcal{N}(\mathcal{T})$	$\mathcal{N}(\mathcal{S})$	$\mathcal{N}(\mathcal{M})$	$\mathcal{N}(\mathcal{L})$	$\mathcal{N}(\mathcal{T})$
alpha (%, annual)	3.68	4.62	3.95	4.64	10.36	6.83	5.71	7.38
	2.04	2.64	2.09	2.50	5.35	3.46	3.07	4.00
dol	-0.55	-0.65	-0.58	-0.62	-0.09	0.06	0.12	0.02
	-13.93	-16.13	-13.63	-15.64	-2.50	1.41	2.89	0.41
car	0.29	0.26	0.26	0.22	0.00	-0.08	-0.03	-0.03
	11.19	6.36	6.05	4.94	0.11	-1.83	-1.01	-0.69
vol	-0.07	-0.01	-0.06	-0.09	-0.26	-0.19	-0.18	-0.23
	-1.76	-0.31	-1.36	-1.95	-7.06	-4.68	-5.48	-6.12
vrp	-0.09	-0.12	-0.06	-0.08	0.02	0.01	0.05	0.03
	-3.21	-3.83	-1.62	-2.31	0.62	0.48	2.13	0.97
mom	0.00	0.09	0.11	0.11	0.15	0.17	0.13	0.16
	0.02	3.16	2.85	2.67	4.69	5.51	4.84	5.26
R^2 (%)	29.31	31.73	28.58	31.92	19.97	14.47	8.80	15.83
Number of obs.	4457	4457	4457	4457	4457	4457	4457	4457

Table 9. Weekly Frequency

This table presents a robustness analysis of currency strategies implemented on a weekly frequency. The table reports descriptive statistics of net-directional network portfolios (Panel A) and benchmark strategies (Panel B), and a contemporaneous regression (Panel C) of the weekly returns of net-directional network portfolios ($\mathcal{N}(\mathcal{H}) : \mathcal{H} \in \{\mathcal{S}, \mathcal{M}, \mathcal{L}, \mathcal{T}\}$) on benchmark strategies - dollar (dol), carry trade (car), volatility (vol), volatility risk premium (vrp), and momentum (mom). In Panels A and B, mean, standard deviation, and Sharpe ratio are annualized, but t-statistic of mean, skewness, kurtosis and the first-order autocorrelation are based on weekly returns. In Panel C, constants reported in the “alpha (% annual)” row are expressed in percentage per annum. The numbers in rows with a grey font are t-statistics of the estimates. The t-statistics are based on [Newey and West \(1987\)](#) standard errors with [Andrews \(1991\)](#) optimal lag selection. The last two rows report adjusted R^2 values (in percentage) and the number of observations. The sample is from January 1996 to December 2013.

Panel A: Performance of network portfolios								
	Total linkages				Causal linkages			
	$\mathcal{N}(\mathcal{S})$	$\mathcal{N}(\mathcal{M})$	$\mathcal{N}(\mathcal{L})$	$\mathcal{N}(\mathcal{T})$	$\mathcal{N}(\mathcal{S})$	$\mathcal{N}(\mathcal{M})$	$\mathcal{N}(\mathcal{L})$	$\mathcal{N}(\mathcal{T})$
mean (%)	4.09	3.60	3.22	4.13	8.70	4.78	4.61	5.35
t-stat	1.90	1.83	1.59	2.03	4.29	2.66	2.79	2.99
Sharpe	0.49	0.42	0.36	0.47	0.99	0.57	0.57	0.64
std (%)	8.41	8.57	8.89	8.78	8.76	8.43	8.09	8.35
skew	-0.12	-0.19	0.56	0.56	1.41	0.89	0.46	0.40
kurt	3.76	4.41	9.75	8.44	20.74	13.54	8.45	9.65
ac1	0.04	-0.06	-0.05	-0.06	-0.05	-0.09	-0.07	-0.11
Panel B: Performance of benchmark strategies								
	dol					car	vol	vrp
	mean (%)	1.61	7.38	0.31	2.58	2.51		
t-stat	0.83	2.96	0.17	1.02	1.02	1.13		
Sharpe	0.20	0.70	0.04	0.24	0.24			
std (%)	7.87	10.59	7.80	10.66	10.66	10.47		
skew	-0.51	-0.82	0.49	0.44	0.44	-0.72		
kurt	6.75	7.87	7.91	6.59	6.59	8.63		
ac1	-0.02	-0.09	-0.03	-0.08	-0.08	-0.15		
Panel C: Returns of network portfolios on benchmark strategies								
	Total linkages				Causal linkages			
	$\mathcal{N}(\mathcal{S})$	$\mathcal{N}(\mathcal{M})$	$\mathcal{N}(\mathcal{L})$	$\mathcal{N}(\mathcal{T})$	$\mathcal{N}(\mathcal{S})$	$\mathcal{N}(\mathcal{M})$	$\mathcal{N}(\mathcal{L})$	$\mathcal{N}(\mathcal{T})$
alpha (% annual)	3.20	2.59	2.18	3.37	7.77	4.23	3.05	4.45
	1.62	1.48	1.15	1.95	3.70	2.09	1.81	2.50
dol	-0.64	-0.62	-0.51	-0.66	-0.13	0.05	0.18	-0.01
	-10.68	-10.54	-9.25	-10.34	-1.74	0.64	2.46	-0.10
car	0.28	0.27	0.23	0.23	0.02	-0.07	0.03	-0.02
	5.98	5.48	3.92	4.36	0.34	-0.89	0.63	-0.30
vol	0.08	-0.01	-0.08	0.03	0.06	0.06	0.06	0.07
	1.10	-0.13	-0.99	0.35	0.95	1.23	1.05	1.33
vrp	-0.09	-0.07	-0.01	-0.05	0.23	0.20	0.27	0.21
	-1.11	-0.97	-0.07	-0.61	3.54	3.02	3.98	3.15
mom	0.02	0.08	0.08	0.10	0.15	0.18	0.13	0.19
	0.48	2.11	1.96	2.14	3.29	4.31	2.31	4.63
R^2 (%)	26.63	28.63	21.69	29.70	18.21	16.36	11.68	18.36
Number of obs.	890	890	890	890	890	890	890	890

net-directional network linkages, but we find that trading medium- and long-term connectedness now becomes more profitable. Third, among the benchmarks, the carry trade is the only strategy consistently generating high Sharpe ratios (0.65 and 0.70 for the daily and weekly frequency).

Finally, the contemporaneous regressions indicate that the estimated alphas exhibit similar patterns to the risk-adjusted performance measured by the Sharpe ratios. Specifically, the abnormal returns of total connectedness strategies relative to the benchmarks seem to increase stronger for longer network horizons than for shorter ones, 2.18% and 3.95% per annum for $\mathcal{N}(\mathcal{L})$ and 3.20% and 3.68% per annum for $\mathcal{N}(\mathcal{S})$ with weekly and daily frequencies, respectively. The alphas of strategies employing causal connectedness strongly increase in magnitude and become highly significant, both economically and statistically: 5.71% per annum (a t-stat of 3.07) for $\mathcal{N}(\mathcal{L})$ and 10.36% per annum (a t-stat of 5.35) for $\mathcal{N}(\mathcal{S})$ with the daily rebalancing.

In sum, the profits of network strategies strongly increase when we move to daily portfolio constructions. The improvement is especially pronounced for causal connectedness. Hence, unlike most of the standard benchmark strategies, investing in currencies based on the network risk information is profitable regardless of trader's investment horizons.

4.5 *Transaction Costs and Subsamples*

We perform two additional robustness checks. First, we report the performance statistics for the network excess returns net of transaction costs. Since the bid-ask quotes for exchange rates are available from Barclays and Reuters, we incorporate those into the currency excess returns following [Menkhoff, Sarno, Schmeling, and Schrimpf \(2012b\)](#).¹⁵ It is worth noting that the bid-ask data are for quoted spreads and not effective spreads. [Lyons et al. \(2001\)](#) suggest that the bid-ask spread data from Reuters are based on the indicative spreads and, therefore, might be too high relative to actual effective ones. Following the existing literature (see, for example, [Goyal and Saretto \(2009\)](#), [Menkhoff, Sarno, Schmeling, and Schrimpf \(2012a, 2017\)](#), and [Colacito, Riddiough, and Sarno \(2020\)](#) among others), we employ 50% of quoted bid-ask spreads in our calculations.¹⁶

¹⁵Please see Appendix C for more details on how we account for transaction costs.

¹⁶[Gilmore and Hayashi \(2011\)](#) suggest that the effective bid-ask spreads could be even lower than 50%, while [Cespa, Gargano, Riddiough, and Sarno \(2019\)](#) suggest a 25% rule for the data from 2011.

Table 10. Transaction Costs

This table presents descriptive statistics for long-short net-directional (Panel A), to-directional and from-directional (Panel B) network portfolios adjusted for transaction costs. Mean, standard deviation, and Sharpe ratio are annualized, but t-statistic of mean, skewness, kurtosis and the first-order autocorrelation are based on monthly returns. The t-statistics are based on [Newey and West \(1987\)](#) standard errors with [Andrews \(1991\)](#) optimal lag selection. The sample is from January 1996 to December 2013.

Panel A: Net-directional network portfolios								
	Total linkages				Causal linkages			
	$\mathcal{N}(\mathcal{S})$	$\mathcal{N}(\mathcal{M})$	$\mathcal{N}(\mathcal{L})$	$\mathcal{N}(\mathcal{T})$	$\mathcal{N}(\mathcal{S})$	$\mathcal{N}(\mathcal{M})$	$\mathcal{N}(\mathcal{L})$	$\mathcal{N}(\mathcal{T})$
mean (%)	4.60	3.26	1.86	3.45	5.37	2.37	1.70	3.88
t-stat	2.06	1.44	0.81	1.52	3.19	1.46	1.14	2.40
Sharpe	0.54	0.39	0.21	0.41	0.66	0.33	0.24	0.52
std (%)	8.49	8.29	8.71	8.43	8.07	7.21	7.07	7.43
skew	-0.41	-0.41	-0.01	-0.30	0.93	0.07	0.02	-0.33
kurt	4.25	4.54	5.12	4.09	6.83	3.41	3.45	4.89
ac1	0.10	0.20	0.09	0.12	-0.15	-0.04	-0.05	-0.04

Panel B: To- and from-directional network portfolios								
	Causal linkages				Causal linkages			
	$\mathcal{T}(\mathcal{S})$	$\mathcal{T}(\mathcal{M})$	$\mathcal{T}(\mathcal{L})$	$\mathcal{T}(\mathcal{T})$	$\mathcal{F}(\mathcal{S})$	$\mathcal{F}(\mathcal{M})$	$\mathcal{F}(\mathcal{L})$	$\mathcal{F}(\mathcal{T})$
mean (%)	5.03	5.46	5.56	4.93	-0.47	0.29	-0.52	1.41
t-stat	3.03	3.09	3.38	2.90	-0.30	0.18	-0.32	0.90
Sharpe	0.61	0.67	0.70	0.61	-0.06	0.04	-0.07	0.19
std (%)	8.28	8.13	7.98	8.04	7.26	7.57	7.22	7.39
skew	0.33	0.23	0.24	0.31	0.03	-0.03	0.01	-0.30
kurt	5.26	3.94	4.02	4.24	3.64	3.91	3.21	4.23
ac1	-0.15	-0.11	-0.19	-0.13	-0.11	-0.04	-0.07	-0.04

Table 10 reports summary statistics of the excess returns of currency network portfolios adjusted for transaction costs. Comparing with the results shown in Tables 1 and 2, the Sharpe ratios of the $\mathcal{N}(\mathcal{S})$ portfolios based on total and causal connectedness decline from 0.65 and 0.80 to 0.54 and 0.66, respectively. The long-short to-directional network portfolios experience a comparable drop in their performances, with the Sharpe ratios ranging from 0.61 to 0.70. Hence, although the returns are somewhat lower after accounting for transaction costs, the network portfolios still exhibit both economically and statistically significant performance.

Second, we divide the whole sample into half and look at the performance of the network strategies for the two subperiods (1996-2004 and 2005-2013). The availability and the amount of currency options vary over time and countries, with sparser data for the first half of the sample. As can be expected, with less precise estimates of the forward-looking currency variances, trading network connectedness is less profitable from 1996 to 2004,

Table 11. Subsamples

This table presents a robustness analysis of currency strategies for the subsamples from January 1996 to December 2004 and from January 2005 to December 2013. The table reports descriptive statistics of net-directional network portfolios from total (Panel A) and causal (Panel B) connectedness. Mean, standard deviation, and Sharpe ratio are annualized, but t-statistic of mean, skewness, kurtosis and the first-order autocorrelation are based on monthly returns. The t-statistics are based on [Newey and West \(1987\)](#) standard errors with [Andrews \(1991\)](#) optimal lag selection.

Panel A: Total linkages								
	1996-2004				2005-2013			
	$\mathcal{N}(\mathcal{S})$	$\mathcal{N}(\mathcal{M})$	$\mathcal{N}(\mathcal{L})$	$\mathcal{N}(\mathcal{T})$	$\mathcal{N}(\mathcal{S})$	$\mathcal{N}(\mathcal{M})$	$\mathcal{N}(\mathcal{L})$	$\mathcal{N}(\mathcal{T})$
mean (%)	5.22	3.73	0.60	3.76	5.83	4.59	4.89	4.92
t-stat	1.51	0.98	0.16	1.01	2.04	1.86	1.99	1.91
Sharpe	0.57	0.39	0.06	0.40	0.73	0.65	0.65	0.67
std (%)	9.08	9.44	9.73	9.40	7.96	7.02	7.54	7.39
skew	-0.11	-0.49	-0.37	-0.52	-0.78	-0.11	0.97	0.25
kurt	2.82	4.42	3.84	3.78	6.52	3.54	7.01	4.12
ac1	0.12	0.25	0.19	0.20	0.07	0.10	-0.09	-0.03
Panel B: Causal linkages								
	1996-2004				2005-2013			
	$\mathcal{N}(\mathcal{S})$	$\mathcal{N}(\mathcal{M})$	$\mathcal{N}(\mathcal{L})$	$\mathcal{N}(\mathcal{T})$	$\mathcal{N}(\mathcal{S})$	$\mathcal{N}(\mathcal{M})$	$\mathcal{N}(\mathcal{L})$	$\mathcal{N}(\mathcal{T})$
mean (%)	6.07	0.30	0.61	2.39	6.79	6.51	4.83	7.37
t-stat	2.25	0.14	0.30	1.00	3.27	2.83	2.28	3.52
Sharpe	0.69	0.04	0.08	0.28	0.92	0.99	0.75	1.18
std (%)	8.74	7.74	7.64	8.45	7.42	6.57	6.43	6.25
skew	0.44	0.09	0.04	-0.45	1.78	0.20	0.08	0.31
kurt	3.61	3.25	2.89	4.76	12.48	3.62	4.34	3.32
ac1	-0.15	-0.14	-0.16	-0.08	-0.15	0.06	0.08	0.02
	1996-2004				2005-2013			
	$\mathcal{T}(\mathcal{S})$	$\mathcal{T}(\mathcal{M})$	$\mathcal{T}(\mathcal{L})$	$\mathcal{T}(\mathcal{T})$	$\mathcal{T}(\mathcal{S})$	$\mathcal{T}(\mathcal{M})$	$\mathcal{T}(\mathcal{L})$	$\mathcal{T}(\mathcal{T})$
mean (%)	6.64	6.38	7.10	6.40	5.57	6.65	6.13	5.59
t-stat	2.56	2.24	2.72	2.29	2.67	3.11	2.98	2.81
Sharpe	0.73	0.69	0.77	0.69	0.76	0.97	0.93	0.83
std (%)	9.15	9.28	9.22	9.23	7.34	6.85	6.58	6.71
skew	0.07	0.10	0.18	0.09	0.86	0.58	0.38	0.85
kurt	3.57	3.52	3.67	3.48	8.70	4.19	3.79	5.53
ac1	-0.15	-0.12	-0.21	-0.12	-0.15	-0.09	-0.14	-0.15

though the short-term net-directional and especially to-directional portfolios still exhibit high Sharpe ratios. With more data available from 2005 to 2013, the network strategies generate the Sharpe ratios ranging from 0.65 to 1.18. In particular, the risk-adjusted return of the causal $\mathcal{N}(\mathcal{S})$ portfolio is 0.92 with a skewness of 1.78 in the second half.

5 Asset Pricing

This section presents the cross-sectional asset-pricing tests performed on the excess returns of network portfolios. Motivated by the previous results, we focus on two sets of test portfolios: the cross-section of currency returns sorted by the short-term net-directional connectedness extracted from total and causal linkages.

5.1 Methodology

Cross-sectional asset pricing tests are based on a stochastic discount factor (SDF) approach (Cochrane, 2005). In our application, we adopt the setting of Lustig, Roussanov, and Verdelhan (2011) for the network portfolios of our paper. In the absence of arbitrage opportunities, the excess returns rx_{t+1}^j of a portfolio j have a zero price and satisfy the following Euler equation:

$$\mathbb{E}_t \left(M_{t+1} rx_{t+1}^j \right) = 0, \quad (11)$$

in which M_{t+1} is the SDF. Following a common approach in the literature, we consider the linear specification of M_{t+1} :

$$M_{t+1} = 1 - b' (f_{t+1} - \mu_f), \quad (12)$$

in which f_{t+1} is the vector of pricing factors, b is the vector of SDF loadings, μ_f is the vector on factor means.¹⁷ Combining Equations (11) and (12), one can obtain a beta pricing model $\mathbb{E}_t \left(rx_{t+1}^j \right) = \lambda' \beta^j$, in which λ is the vector of the factor risk prices, and β^j is the vector of the risk quantities. The latter are also the regression coefficients of excess returns rx_{t+1}^j on the risk factors f_{t+1} . Further, the SDF loadings and factor risk prices are related to each other via the equation $\lambda = \Sigma_f b$, where $\Sigma_f = \mathbb{E}_t \left[(f_{t+1} - \mu_f) (f_{t+1} - \mu_f)' \right]$ is the variance-covariance matrix of the risk factors.

We test a variety of linear factor models for the cross-section of network portfolios. For each model specification, we estimate the factor loadings via the one-step generalized method of moments (GMM) with the identity weighting matrix (Hansen, 1982). We simultaneously estimate the unknown factor means by adding the corresponding restrictions to a set of moments for the pricing errors. Since we are interested in testing whether a partic-

¹⁷Other prominent examples considering a linear SDF specification include Menkhoff, Sarno, Schmeling, and Schrimpf (2012a), Della Corte, Ramadorai, and Sarno (2016), Colacito, Riddiough, and Sarno (2020) and Della Corte, Kozhan, and Neuberger (2020) among many others.

ular linear model explains the cross-section of expected currency excess returns, we implement a GMM estimation based on unconditional moments without instruments. Having estimated SDF loadings, we recover the risk prices from the identity $\lambda = \Sigma_f b$ and calculate their standard errors using the Delta method. The t-statistics of b 's and λ 's are based on [Newey and West \(1987\)](#) standard errors with [Andrews \(1991\)](#) optimal lag selection. We evaluate the fit of the linear pricing models by using three statistics: the cross-sectional R^2 , root mean squared pricing error (RMSE), and the [Hansen and Jagannathan \(1997\)](#) distance (HJ_{dist}). We further calculate the simulated p-values for testing the null hypothesis that the pricing errors equal zero, i.e. HJ_{dist} equals zero. Following [Jagannathan and Wang \(1996\)](#) and [Kan and Robotti \(2008\)](#), we obtain the simulated p-values by using a weighted sum of independent random variables from $\chi^2(1)$ distribution.¹⁸

5.2 Principal Component Analysis on Network Portfolios

Before performing formal cross-sectional asset pricing tests, we investigate whether average network excess returns stemming from the predictability of short-term net-directional connectedness can be associated with a small group of risk factors. Following [Lustig, Rousanov, and Verdelhan \(2011\)](#), we conduct a principal component (PC) decomposition of the currency returns sorted on network risk measures extracted from total and causal linkage. Further, we study the correlations of the principal components with the corresponding long-short network portfolios and benchmark strategies.

Table 12 presents the results. There are several common and distinctive features of the two cross-sections. First, the PC loadings indicate a strong factor structure in both groups of currency portfolios. The first principal component (PC1) accounts for most of the time-variation in quintile portfolios and has similar loadings across the five portfolios. The second principal component (PC2) in turn displays a pronounced monotonic pattern in loadings as we move from \mathcal{P}_1 to \mathcal{P}_5 : the increasing and decreasing tendencies for total and causal linkages. Second, the first two principal components explain around 84% and 86% of the common variation in network portfolios with total and causal connections. Further, they exhibit similar correlations with the risk factors. PC1 is perfectly correlated with the dollar factor in both cases. PC2 exhibits the strongest correlation with the long-short network portfolio, though the relationship is of the opposite sign in the two cases.

¹⁸ Appendix B provides a detailed description of the GMM estimation and test statistics.

Table 12. Principal Components: Short-term Net-directional Network Portfolios

This table presents the loadings of principal components ($PC_i : i = 1, \dots, 5$) for quintile portfolios ($\mathcal{P}_i : i = 1, \dots, 5$) sorted by short-term net-directional connectedness extracted from total (Panel A) and causal (Panel B) linkages. Each panel also reports correlations of the principal components with a long-short network portfolio ($\mathcal{N}(\mathcal{S})$) and benchmark strategies - dollar (dol), carry trade (car), volatility (vol), volatility risk premium (vrp), and momentum (mom). The sample is from January 1996 to December 2013.

Panel A: Total linkages												
	PC loadings						Correlations					
	\mathcal{P}_1	\mathcal{P}_2	\mathcal{P}_3	\mathcal{P}_4	\mathcal{P}_5	CV	$\mathcal{N}(\mathcal{S})$	dol	car	vol	vrp	mom
PC1	0.53	0.52	0.44	0.38	0.32	76.03	-0.46	1.00	0.30	0.59	-0.05	0.00
PC2	-0.49	-0.43	0.35	0.60	0.32	84.34	0.58	0.05	0.47	0.19	-0.25	-0.01
PC3	-0.05	-0.04	-0.13	-0.46	0.87	90.85	0.59	0.04	0.06	0.07	-0.09	0.22
PC4	-0.10	-0.09	0.82	-0.53	-0.17	96.30	-0.04	-0.01	-0.07	0.15	-0.15	-0.07
PC5	-0.68	0.73	-0.02	-0.01	-0.02	100.00	0.32	-0.01	0.07	-0.07	-0.08	0.04

Panel B: Causal linkages												
	PC loadings						Correlations					
	\mathcal{P}_1	\mathcal{P}_2	\mathcal{P}_3	\mathcal{P}_4	\mathcal{P}_5	CV	$\mathcal{N}(\mathcal{S})$	dol	car	vol	vrp	mom
PC1	0.45	0.50	0.47	0.47	0.34	77.62	-0.26	1.00	0.32	0.60	-0.06	0.01
PC2	0.88	-0.15	-0.20	-0.36	-0.17	86.16	-0.79	0.01	0.18	0.06	-0.20	-0.06
PC3	0.07	-0.47	-0.32	0.18	0.80	92.08	0.46	0.04	0.31	0.11	-0.21	0.13
PC4	0.13	-0.42	-0.10	0.76	-0.47	96.27	-0.31	-0.01	0.01	0.00	-0.06	-0.01
PC5	0.01	-0.58	0.79	-0.20	0.02	100.00	0.01	0.00	-0.10	0.09	0.09	-0.12

In relative terms, under the causal linkages, the correlation of PC2 with $\mathcal{N}(\mathcal{S})$ is strongly dominant, whereas PC2 from total connectedness almost equally correlate with $\mathcal{N}(\mathcal{S})$ and the carry trade factor. Finally, the starker difference between the two portfolio groups is related to loadings of the third principal component (PC3), which show no visible pattern in Panel A but display the monotonicity in Panel B. In the latter case, PC3 strongly relates to the network and carry trade risk factors.

Overall, the results, presented in Table 12, suggest that the network-sorted portfolios indeed can be summarized by a small number of risk factors. We can approximate the first using the average returns across spot currency portfolios and interpret it as a “level” factor. We can approximate the second using the spread between \mathcal{P}_5 and \mathcal{P}_1 portfolios and interpret it as a “level” factor. In case of causal connectedness portfolios, the results are suggestive of an additional “level” factor, which is strongly correlated with the carry trade.

5.3 Cross-Sectional Regressions

We now turn to the formal investigation of our network portfolios following the methodology outlined in Section 5.1. Motivated by the principal component analysis in Section

5.2, we consider (A1) a variety of two-factor linear models for the cross-section of excess returns sorted on total connectedness and (A2) a variety of two- and three-factor linear models for the test excess returns sorted on causal connectedness. In particular, the two-factor SDFs has dol as the first factor plus a second factor, including car, vol, vrp, mom, and $\mathcal{N}(\mathcal{S})$. For the three-factor SDFs, we start with the two factors, dol and $\mathcal{N}(\mathcal{S})$, and then consider various third factors, including car, vol, vrp, and mom.

Table 13 presents the asset pricing results for all models considered, with Panel A showing the specifications in (A1), and Panels B and C reporting the frameworks in (A2). The results in Panel A indicate that none of the SDF loadings and risk prices for benchmark risk factors are statistically significant at 5% level. In contrast, we document the positive and statistically significant loading (a t-stat of 2.38) and price (a t-stat of 2.15) of the network risk factor. In particular, the GMM estimate of $\lambda_{\mathcal{N}(\mathcal{S})}$ is 0.47% per month. Since the network factor is actually tradable, we can apply the Euler equation to the factor excess returns and derive that its price of risk must be equal to the average excess return. Using statistics reported in Table 1, we verify that this no-arbitrage condition indeed holds: the monthly average return of 0.46% is close to the estimated price of 0.47%. Regarding the dollar factor, its SDF loading and price of risk are insignificant at conventional confidence levels (a t-stat of 1.21 for b_{dol} and a t-stat of 0.66 for λ_{dol}). Moreover, the estimated λ_{dol} matches factor's average excess return of 0.13% per month as reported in Table 3. Even though the dollar factor does not help to explain the average excess returns, it serves as a constant capturing the common mispricing in the cross-sectional regression.

In terms of the model fit, the two-factor SDFs combining the dollar and other benchmark risk factors produce similar performances, capturing from 32.61% to 47.06% of total variance in the cross-sectional returns and yielding RMSEs from 0.11% to 0.14%. One also cannot reject any of these linear model based on HJ_{dist} because the simulated p-values are far above 50% in all cases. At the same time, the SDF specification comprising the dollar and network risk factors outperforms other models by a large margin. For instance, it generates more than twice-as-large cross-sectional R^2 of 97.18% and more than three times smaller RMSE and HJ_{dist} of 0.03% and 0.05.

In sum, the benchmark risk factors from the existing literature have a hard time ex-

Table 13. Pricing Short-term Net-directional Network Portfolios

This table presents cross-sectional asset pricing results. We price quintile portfolios ($\mathcal{P}_i : i = 1, \dots, 5$) sorted by short-term net-directional connectedness. In Panels A and B, we construct two-factor linear SDFs with the dollar (dol) factor plus a second factor, including carry trade (car), volatility (vol), volatility risk premium (vrp), momentum (mom), and short-term net-directional network ($\mathcal{N}(\mathcal{S})$) factors. In Panel C, we construct three-factor linear SDFs with dol, $\mathcal{N}(\mathcal{S})$ plus a third factor, including car, vol, vrp, and mom. Each panel reports one-step GMM estimates of factor loadings (b) and prices of factor risks (λ). Goodness-of-fit statistics include the R^2 and root mean squared pricing error (RMSE) (both are expressed in percentage), and the [Hansen and Jagannathan \(1997\)](#) distance (HJ_{dist}) with simulated p-values in parentheses. The p-values are for the null hypothesis that the pricing errors are equal to zero. The remaining numbers in rows with a grey font are t-statistics of the estimates, which are based on [Newey and West \(1987\)](#) standard errors with [Andrews \(1991\)](#) optimal lag selection. The sample is from January 1996 to December 2013.

Panel A: Total linkages: two-factor models

	SDF loadings		Risk prices		Model fit		
	b_{dol}	b_{f_2}	λ_{dol}	λ_{f_2}	R^2 (%)	RMSE (%)	HJ_{dist}
dol + car	−0.03	0.12	0.12	1.02	47.06	0.11	0.16
	−0.55	1.73	0.50	1.78			(0.75)
dol + vol	−0.14	0.25	0.12	1.12	23.00	0.14	0.21
	−1.10	1.33	0.64	1.43			(0.58)
dol + vrp	0.01	−0.25	0.12	−1.33	49.11	0.11	0.16
	0.11	−1.46	0.48	−1.47			(0.78)
dol + mom	0.02	0.26	0.12	1.94	32.61	0.13	0.16
	0.35	1.57	0.40	1.57			(0.80)
dol + $\mathcal{N}(\mathcal{S})$	0.07	0.10	0.13	0.47	97.18	0.03	0.05
	1.55	2.38	0.66	2.15			(0.99)

Panel B: Causal linkages: two-factor models

dol + car	−0.03	0.12	0.12	1.00	4.90	0.20	0.32
	−0.49	1.44	0.51	1.52			(0.42)
dol + vol	−0.22	0.37	0.12	1.63	1.79	0.20	0.33
	−0.96	1.07	0.62	1.12			(0.46)
dol + vrp	0.02	−0.07	0.11	−0.40	−9.82	0.21	0.35
	0.40	−0.67	0.55	−0.69			(0.29)
dol + mom	0.02	0.43	0.12	3.19	32.04	0.17	0.30
	0.25	1.94	0.31	1.94			(0.71)
dol + $\mathcal{N}(\mathcal{S})$	0.04	0.09	0.12	0.43	40.72	0.16	0.25
	1.21	2.89	0.66	2.92			(0.47)

Panel C: Causal linkages: three-factor models

	SDF loadings			Risk prices			Model fit		
	b_{dol}	b_{f_2}	$b_{\mathcal{N}(\mathcal{S})}$	λ_{dol}	λ_{f_2}	$\lambda_{\mathcal{N}(\mathcal{S})}$	R^2 (%)	RMSE (%)	HJ_{dist}
dol + car + $\mathcal{N}(\mathcal{S})$	−0.02	0.15	0.10	0.13	1.32	0.48	71.94	0.11	0.19
	−0.33	1.84	2.89	0.54	1.87	2.72			(0.69)
dol + vol + $\mathcal{N}(\mathcal{S})$	−0.01	0.18	0.10	0.12	0.85	0.45	56.81	0.13	0.22
	−0.41	0.64	2.58	0.70	0.70	2.58			(0.58)
dol + vrp + $\mathcal{N}(\mathcal{S})$	0.04	−0.23	0.11	0.13	−1.21	0.46	66.06	0.12	0.21
	0.83	−1.51	2.57	0.61	−1.49	2.37			(0.67)
dol + mom + $\mathcal{N}(\mathcal{S})$	0.03	0.19	0.06	0.12	1.49	0.44	45.45	0.15	0.25
	0.71	0.83	2.06	0.48	0.87	2.12			(0.58)

plaining the network-sorted portfolios, whereas the network risk factor successfully prices the novel cross-section of currency returns documented in our paper. Furthermore, the quantitative results show a significant wedge in the contribution of the network and other factors, despite possible common components in their returns originating from the interest rate predictability (for car), contemporaneous correlations in spot variances (for vol) or spot implied variances (for vrp).

Panel B in Table 13 shows the results for network portfolios sorted on the causal connectedness measure. As can be expected, once we eliminate the contemporaneous effects in the currency uncertainty network, the performance of the SDFs with car, vol and vrp risk factors deteriorates significantly. The t-statistics of SDF loadings and factor prices become even smaller in absolute terms. Further, the R^2 statistics drop dramatically to 4.90% and 1.79% with car and vol as a second factor or become negative -9.82% in case of vrp. Interestingly, the performance of the linear model with dol and mom remains the same, though the evidence on priced momentum risk is weak. In contrast, the factor loading and price of network risk become statistically significant at 1% level (a t-stat of 2.89 for $b_{\mathcal{N}(\mathcal{S})}$ and a t-stat of 2.92 for $\lambda_{\mathcal{N}(\mathcal{S})}$). The model involving the network factor also displays stronger explanatory power as measured by higher R^2 (40.72%) and generates the lower pricing errors as measured by lower RMSE (0.16%) and HJ_{dist} (0.25).

In Panel C in Table 13, we extend the model with dol and $\mathcal{N}(\mathcal{S})$ to the three-factor specification with car, vol, vrp or mom. The inclusion of an additional factor generally leads to higher R^2 , lower RMSE and HJ_{dist} statistics relative to the original two-factor SDF. Most importantly, the network risk remains strongly priced in all specifications. Further, consistent with the principal component decomposition, the best-performing three-factor model includes the dollar, carry trade and network risk factors. Overall, the results emphasize the importance of the network risk factors extracted from total and especially causal currency connectedness in explaining the novel cross-sections of currency returns. These excess returns cannot be understood through the lens of the benchmark factors.

5.4 Time-series Exposure to Network Factors

We further estimate the sensitivity of the excess returns of quintile portfolios ($\mathcal{P}_i : i = 1, \dots, 5$) to the network risk. Table 14 reports the outputs of a contemporaneous regression

Table 14. Net-directional Network Portfolios: Factor Betas

This table presents a contemporaneous regression of monthly excess returns of each quintile portfolio on two risk factors - the dollar and short-term net-directional network portfolios (Panel A), and on three risk factors - the dollar, carry/volatility, and short-term net-directional network portfolios (Panel B). Constants reported in the “alpha (%, annual)” row are expressed in percentage per annum. The numbers in rows with a grey font are t-statistics of the estimates, which are based on [Newey and West \(1987\)](#) standard errors with [Andrews \(1991\)](#) optimal lag selection. The last row in each panel shows the adjusted R^2 (in percentage). The sample is from January 1996 to December 2013.

Panel A: Short-term net-directional portfolios

	Total linkages					Causal linkages				
	\mathcal{P}_1	\mathcal{P}_2	\mathcal{P}_3	\mathcal{P}_4	\mathcal{P}_5	\mathcal{P}_1	\mathcal{P}_2	\mathcal{P}_3	\mathcal{P}_4	\mathcal{P}_5
alpha (%, annual)	0.34	-0.40	-0.13	-0.31	0.34	2.16	-1.03	-0.77	-2.74	2.16
	0.58	-0.32	-0.12	-0.21	0.58	3.11	-0.91	-0.76	-2.96	3.11
β_{dol}	0.99	1.09	1.01	0.91	0.99	0.88	1.11	1.05	1.08	0.88
	36.16	18.79	21.65	16.71	36.16	32.55	27.67	33.20	25.22	32.55
$\beta_{\mathcal{N}(\mathcal{S})}$	-0.47	-0.18	0.03	0.05	0.53	-0.57	0.00	0.03	0.13	0.43
	-19.84	-3.65	0.65	0.91	22.18	-15.34	0.07	0.91	3.37	11.39
$R^2(\%)$	94.26	83.70	75.81	67.35	89.51	91.66	82.70	82.06	81.92	86.37

Panel B: Short-term net-directional portfolios: causal linkages

	car					vol				
	\mathcal{P}_1	\mathcal{P}_2	\mathcal{P}_3	\mathcal{P}_4	\mathcal{P}_5	\mathcal{P}_1	\mathcal{P}_2	\mathcal{P}_3	\mathcal{P}_4	\mathcal{P}_5
alpha (%, annual)	1.49	-0.48	0.02	-2.67	1.49	2.10	-0.91	-0.78	-2.72	2.10
	2.29	-0.42	0.02	-2.74	2.29	3.02	-0.81	-0.76	-2.91	3.02
β_{dol}	0.84	1.14	1.10	1.09	0.84	0.85	1.17	1.04	1.10	0.85
	28.44	27.04	31.17	24.51	28.44	22.04	22.56	24.04	20.79	22.04
β_{f_2}	0.10	-0.08	-0.12	-0.01	0.10	0.04	-0.09	0.01	-0.02	0.04
	3.27	-1.91	-3.79	-0.42	3.27	1.06	-1.72	0.11	-0.53	1.06
$\beta_{\mathcal{N}(\mathcal{S})}$	-0.57	0.00	0.03	0.13	0.43	-0.57	0.00	0.03	0.13	0.43
	-14.79	0.04	0.87	3.37	11.05	-15.72	0.05	0.91	3.36	11.69
$R^2(\%)$	92.67	83.37	83.64	81.93	88.02	91.75	83.15	82.06	81.95	86.52

of excess returns of each quintile portfolio on the dollar and network risk factors (Panel A) and on the dollar, carry trade/volatility, and network risk factors (Panel B).

For the currency returns sorted on total network connectedness, the estimated alphas are statistically insignificant. The β_{dol} coefficients are statistically indistinguishable from one. The β_{net} coefficients display a pronounced monotonicity when we move from \mathcal{P}_1 to \mathcal{P}_5 , increasing from -0.47 (a t-stat of -19.84) to 0.53 (a t-stat of 22.18). The two factors capture a lot of variation of quintile portfolios ranging from 67.35% for \mathcal{P}_4 to 94.26% for \mathcal{P}_1 .

For the currency returns sorted on causal network connectedness, the right part of Panel A and Panel B report the outputs for the two- and three-factor regressions. The results sug-

gest that the first, fourth and fifth portfolios have statistically significant alphas. The size and the degree of significance of alphas are generally reduced when we include additional risk factors, with the impact being particularly large for the inclusion of the carry trade. This can be explained by the observation that the exposure to the volatility factor is statistically insignificant for all portfolios, while the beta estimates for the carry trade are significant for three excess returns. The the goodness of fit and slope coefficients of the network risk factor remain largely unchanged for the two- and three-factor regressions.

Overall, the results of the time-series regressions are consistent with the cross-sectional regressions. Specifically, they reinforce the conclusion that the dollar and network risk factors fully explain the sources of risk in the cross-section of total and causal connectedness portfolios, while the inclusion of the carry trade into a set of factors improves the representation of risks in causal connectedness portfolios.

6 Conclusion

We show that connectedness risk among implied variances on exchange rates predicts currency returns. A long-short portfolio strategy, which buys currencies receiving short-term shocks and sells currencies transmitting short-term shocks, generates a high Sharpe ratio and yields a significant alpha when controlling for popular foreign exchange benchmarks. Trading currency connectedness at longer horizons is less profitable, indicating a downward-sloping term structure of uncertainty network risk in currency markets. A risk factor - an uncertainty network strategy - fully explains the cross-sectional variation of network-sorted excess returns, which cannot be understood through the lens of the existing risk factors - dollar, carry trade, volatility, variance risk premium and momentum. In robustness checks, we show that the performance of network portfolios in terms of risk-adjusted (Sharpe ratios) and benchmark adjusted (estimated alphas) actually improves when the strategies are implemented at daily or weekly frequencies. The significance of monthly network excess returns is robust to transaction costs and subperiods.

Overall, the results of our paper provide new insights into the sources of currency predictability. We do not provide possible explanations for the returns and hence developing a formal theoretical model, which can rationalize our empirical findings, remains an open question. The common international linkages based on trade and cash-flow channels,

which have been proposed to mainly explain the carry trade, are unlikely to capture the network returns, which remain uncorrelated with the popular currency factors. We leave such an interesting and important avenue for future research.

References

Akram, Q. F., D. Rime, and L. Sarno (2008). Arbitrage in the foreign exchange market: Turning on the microscope. *Journal of International Economics* 76(2), 237–253.

Andersen, L., D. Duffie, and Y. Song (2019). Funding value adjustments. *The Journal of Finance* 74(1), 145–192.

Andrews, D. W. (1991). Heteroskedasticity and autocorrelation consistent covariance matrix estimation. *Econometrica: Journal of the Econometric Society*, 817–858.

Asness, C. S., T. J. Moskowitz, and L. H. Pedersen (2013). Value and momentum everywhere. *The Journal of Finance* 68(3), 929–985.

Bakshi, G., N. Kapadia, and D. Madan (2003). Stock return characteristics, skew laws, and the differential pricing of individual equity options. *The Review of Financial Studies* 16(1), 101–143.

Bansal, R. and A. Yaron (2004). Risks for the long run: A potential resolution of asset pricing puzzles. *The Journal of Finance* 59 (4), 1481–1509.

Barunik, J. and M. Ellington (2020). Dynamic networks in large financial and economic systems. *arXiv preprint arXiv:2007.07842*.

BIS (2019a). Otc derivatives statistics at end-june 2019. *Bank for International Settlements, Basel*.

BIS (2019b). Triennial central bank survey of foreign exchange and otc derivatives markets activity in 2019. *Bank for International Settlements, Basel*.

Britten-Jones, M. and A. Neuberger (2000). Option prices, implied price processes, and stochastic volatility. *Journal of Finance* 55, 839–866.

Cespa, G., A. Gargano, S. J. Riddiough, and L. Sarno (2019). Foreign exchange volume. *Unpublished working paper. City University London, University of Cambridge, and The University of Melbourne*.

Chernov, M., J. Graveline, and I. Zviadadze (2018). Crash risk in currency returns. *Journal of Financial and Quantitative Analysis* 53(1), 137–170.

Cochrane, J. H. (2005). *Asset pricing*. Princeton university press.

Colacito, R., M. M. Croce, F. Gavazzoni, and R. Ready (2018). Currency risk factors in a recursive multicountry economy. *The Journal of Finance* 73(6), 2719–2756.

Colacito, R., S. J. Riddiough, and L. Sarno (2020). Business cycles and currency returns.

Journal of Financial Economics.

Corte, P. D., S. J. Riddiough, and L. Sarno (2016). Currency premia and global imbalances. *The Review of Financial Studies* 29(8), 2161–2193.

Dahlhaus, R. (1996). On the kullback-leibler information divergence of locally stationary processes. *Stochastic processes and their applications* 62(1), 139–168.

Dahlhaus, R., W. Polonik, et al. (2009). Empirical spectral processes for locally stationary time series. *Bernoulli* 15(1), 1–39.

Dahlquist, M. and H. Hasseltoft (2020). Economic momentum and currency returns. *Journal of Financial Economics* 136(1), 152–167.

Della Corte, P., R. Kozhan, and A. Neuberger (2020). The cross-section of currency volatility premia. *Journal of Financial Economics*.

Della Corte, P., T. Ramadorai, and L. Sarno (2016). Volatility risk premia and exchange rate predictability. *Journal of Financial Economics* 120(1), 21–40.

Dew-Becker, I., S. Giglio, A. Le, and M. Rodriguez (2017). The price of variance risk. *Journal of Financial Economics* 123(2), 225–250.

Diebold, F. X. and K. Yilmaz (2014). On the network topology of variance decompositions: Measuring the connectedness of financial firms. *Journal of Econometrics* 182(1), 119–134.

Du, W., A. Tepper, and A. Verdelhan (2018). Deviations from covered interest rate parity. *The Journal of Finance* 73(3), 915–957.

Elliott, M., B. Golub, and M. O. Jackson (2014). Financial networks and contagion. *American Economic Review* 104(10), 3115–53.

Farhi, E., S. P. Fraiberger, X. Gabaix, R. Ranciere, and A. Verdelhan (2015). Crash risk in currency markets. Technical report, New York University, New York, NY.

Gabaix, X. and M. Maggiori (2015). International liquidity and exchange rate dynamics. *The Quarterly Journal of Economics* 130(3), 1369–1420.

Garman, M. B. and S. W. Kohlhagen (1983). Foreign currency option values. *Journal of International Money and Finance* 2(3), 231–237.

Gilmore, S. and F. Hayashi (2011). Emerging market currency excess returns. *American Economic Journal: Macroeconomics* 3(4), 85–111.

Glasserman, P. and H. P. Young (2016). Contagion in financial networks. *Journal of Economic Literature* 54(3), 779–831.

Goyal, A. and A. Saretto (2009). Cross-section of option returns and volatility. *Journal of Financial Economics* 94(2), 310–326.

Hansen, L. P. (1982). Large sample properties of generalized method of moments estimators. *Econometrica: Journal of the Econometric Society*, 1029–1054.

Hansen, L. P. and R. Jagannathan (1997). Assessing specification errors in stochastic discount factor models. *The Journal of Finance* 52(2), 557–590.

Herskovic, B. (2018). Networks in production: Asset pricing implications. *The Journal of Finance* 73(4), 1785–1818.

Jagannathan, R. and Z. Wang (1996). The conditional capm and the cross-section of expected returns. *The Journal of finance* 51(1), 3–53.

Jurek, J. W. (2014). Crash-neutral currency carry trades. *Journal of Financial Economics* 113(3), 325–347.

Kadiyala, K. R. and S. Karlsson (1997). Numerical methods for estimation and inference in Bayesian VAR-models. *Journal of Applied Econometrics* 12(2), 99–132.

Kan, R. and C. Robotti (2008). Specification tests of asset pricing models using excess returns. *Journal of Empirical Finance* 15(5), 816–838.

Lustig, H., N. Roussanov, and A. Verdelhan (2011). Common risk factors in currency markets. *The Review of Financial Studies* 24(11), 3731–3777.

Lustig, H. and A. Verdelhan (2007). The cross section of foreign currency risk premia and consumption growth risk. *American Economic Review* 97(1), 89–117.

Lütkepohl, H. (2005). *New introduction to multiple time series analysis*. Springer Science & Business Media.

Lyons, R. K. et al. (2001). *The microstructure approach to exchange rates*, Volume 333. Citeseer.

Menkhoff, L., L. Sarno, M. Schmeling, and A. Schrimpf (2012a). Carry trades and global foreign exchange volatility. *The Journal of Finance* 67(2), 681–718.

Menkhoff, L., L. Sarno, M. Schmeling, and A. Schrimpf (2012b). Currency momentum strategies. *Journal of Financial Economics* 106(3), 660–684.

Menkhoff, L., L. Sarno, M. Schmeling, and A. Schrimpf (2017). Currency value. *The Review of Financial Studies* 30(2), 416–441.

Mueller, P., A. Stathopoulos, and A. Vedolin (2017). International correlation risk. *Journal of Financial Economics* 126(2), 270–299.

Newey, W. and K. West (1987). A simple, positive semi-definite, heteroskedasticity and autocorrelation consistent covariance matrix. *Econometrica*, 703–708.

Pesaran, H. H. and Y. Shin (1998). Generalized impulse response analysis in linear multivariate models. *Economics letters* 58(1), 17–29.

Petrova, K. (2019). A quasi-Bayesian local likelihood approach to time varying parameter VAR models. *Journal of Econometrics*.

Rambachan, A. and N. Shephard (2019). Econometric analysis of potential outcomes time series: instruments, shocks, linearity and the causal response function. *arXiv preprint arXiv:1903.01637*.

Richmond, R. J. (2019). Trade network centrality and currency risk premia. *The Journal of Finance* 74(3), 1315–1361.

Zviadadze, I. (2017). Term structure of consumption risk premia in the cross section of currency returns. *The Journal of Finance* 72(4), 1529–1566.

Appendix for

“Uncertainty Network Risk and Currency Returns”

Abstract

This appendix presents supplementary details not included in the main body of the paper.

Contents

A. Estimation of the time-varying parameter VAR model	50
B. Asset Pricing Tests	52
C. Transaction Costs	54

A Estimation of the time-varying parameter VAR model

Let \mathbf{CIV}_t be an $N \times 1$ vector generated by a stable time-varying parameter (TVP) heteroskedastic VAR model with p lags:

$$\mathbf{CIV}_{t,T} = \boldsymbol{\Phi}_1(t/T)\mathbf{CIV}_{t-1,T} + \dots + \boldsymbol{\Phi}_p(t/T)\mathbf{CIV}_{t-p,T} + \boldsymbol{\epsilon}_{t,T}, \quad (\text{A.1})$$

where $\boldsymbol{\epsilon}_{t,T} = \boldsymbol{\Sigma}^{-1/2}(t/T)\boldsymbol{\eta}_{t,T}$, $\boldsymbol{\eta}_{t,T} \sim NID(0, \mathbf{I}_M)$ and $\boldsymbol{\Phi}(t/T) = (\boldsymbol{\Phi}_1(t/T), \dots, \boldsymbol{\Phi}_p(t/T))^\top$ are the time varying autoregressive coefficients. Note that all roots of the polynomial, $\chi(z) = \det(\mathbf{I}_N - \sum_{p=1}^L z^p \mathbf{B}_{p,t})$, lie outside the unit circle, and $\boldsymbol{\Sigma}_t^{-1}$ is a positive definite time-varying covariance matrix. Stacking the time-varying intercepts and autoregressive matrices in the vector $\boldsymbol{\phi}_{t,T}$ with $\overline{\mathbf{CIV}}_t^\top = (\mathbf{I}_N \otimes \mathbf{x}_t)$, $\mathbf{x}_t = (1, \mathbf{x}_{t-1}^\top, \dots, \mathbf{x}_{t-p}^\top)$ and denoting the Kronecker product by \otimes , the model can be written as:

$$\mathbf{CIV}_{t,T} = \overline{\mathbf{CIV}}_{t,T}^\top \boldsymbol{\phi}_{t,T} + \boldsymbol{\Sigma}_{t/T}^{-\frac{1}{2}} \boldsymbol{\eta}_{t,T} \quad (\text{A.2})$$

We obtain the time-varying parameters of the model by employing the Quasi-Bayesian Local-Likelihood (QBLL) approach of [Petrova \(2019\)](#). The estimation of Equation (A.1) requires re-weighting the likelihood function. The weighting function gives higher proportions to observations surrounding the time period whose parameter values are of interest. The local likelihood function at time period k is given by:

$$\begin{aligned} L_k(\mathbf{CIV} | \theta_k, \boldsymbol{\Sigma}_k, \overline{\mathbf{CIV}}) &\propto \\ |\boldsymbol{\Sigma}_k|^{\text{trace}(\mathbf{D}_k)/2} \exp \left\{ -\frac{1}{2} (\mathbf{CIV} - \overline{\mathbf{CIV}}^\top \boldsymbol{\phi}_k)^\top (\boldsymbol{\Sigma}_k \otimes \mathbf{D}_k) (\mathbf{CIV} - \overline{\mathbf{CIV}}^\top \boldsymbol{\phi}_k) \right\} \end{aligned} \quad (\text{A.3})$$

The \mathbf{D}_k is a diagonal matrix whose elements hold the weights:

$$\mathbf{D}_k = \text{diag}(\varrho_{k1}, \dots, \varrho_{kT}) \quad (\text{A.4})$$

$$\varrho_{kt} = \phi_{T,k} w_{kt} / \sum_{t=1}^T w_{kt} \quad (\text{A.5})$$

$$w_{kt} = (1/\sqrt{2\pi}) \exp((-1/2)((k-t)/H)^2), \quad \text{for } k, t \in \{1, \dots, T\} \quad (\text{A.6})$$

$$\zeta_{Tk} = \left(\left(\sum_{t=1}^T w_{kt} \right)^2 \right)^{-1} \quad (\text{A.7})$$

where ϱ_{kt} is a normalised kernel function. w_{kt} uses a Normal kernel weighting function.

ζ_{Tk} gives the rate of convergence and behaves like the bandwidth parameter H in (A.6). The kernel function puts a greater weight on the observations surrounding the parameter estimates at time k relative to more distant observations.

We use a Normal-Wishart prior distribution for $\phi_k | \Sigma_k$ for $k \in \{1, \dots, T\}$:

$$\phi_k | \Sigma_k \sim \mathcal{N} \left(\phi_{0k}, (\Sigma_k \otimes \Xi_{0k})^{-1} \right) \quad (\text{A.8})$$

$$\Sigma_k \sim \mathcal{W} (\alpha_{0k}, \Gamma_{0k}) \quad (\text{A.9})$$

where ϕ_{0k} is a vector of prior means, Ξ_{0k} is a positive definite matrix, α_{0k} is a scale parameter of the Wishart distribution (\mathcal{W}), and Γ_{0k} is a positive definite matrix.

The prior and weighted likelihood function implies a Normal-Wishart quasi posterior distribution for $\phi_k | \Sigma_k$ for $k = \{1, \dots, T\}$. Formally, let $\mathbf{A} = (\bar{x}_1^\top, \dots, \bar{x}_T^\top)^\top$ and $\mathbf{Y} = (x_1, \dots, x_T)^\top$, then:

$$\phi_k | \Sigma_k, \mathbf{A}, \mathbf{Y} \sim \mathcal{N} \left(\tilde{\theta}_k, (\Sigma_k \otimes \tilde{\Xi}_k)^{-1} \right) \quad (\text{A.10})$$

$$\Sigma_k \sim \mathcal{W} (\tilde{\alpha}_k, \tilde{\Gamma}_k^{-1}) \quad (\text{A.11})$$

with quasi posterior parameters

$$\tilde{\phi}_k = \left(\mathbf{I}_N \otimes \tilde{\Xi}_k^{-1} \right) \left[\left(\mathbf{I}_N \otimes \mathbf{A}^\top \mathbf{D}_k \mathbf{A} \right) \hat{\phi}_k + \left(\mathbf{I}_N \otimes \Xi_{0k} \right) \phi_{0k} \right] \quad (\text{A.12})$$

$$\tilde{\Xi}_k = \tilde{\Xi}_{0k} + \mathbf{A}^\top \mathbf{D}_k \mathbf{A} \quad (\text{A.13})$$

$$\tilde{\alpha}_k = \alpha_{0k} + \sum_{t=1}^T \varrho_{kt} \quad (\text{A.14})$$

$$\tilde{\Gamma}_k = \Gamma_{0k} + \mathbf{Y}' \mathbf{D}_k \mathbf{Y} + \Phi_{0k} \Gamma_{0k} \Phi_{0k}^\top - \tilde{\Phi}_k \tilde{\Gamma}_k \tilde{\Phi}_k^\top \quad (\text{A.15})$$

where $\hat{\phi}_k = (\mathbf{I}_N \otimes \mathbf{A}^\top \mathbf{D}_k \mathbf{A})^{-1} (\mathbf{I}_N \otimes \mathbf{A}^\top \mathbf{D}_k) y$ is the local likelihood estimator for ϕ_k . The matrices Φ_{0k} , $\tilde{\Phi}_k$ are conformable matrices from the vector of prior means, ϕ_{0k} , and a draw from the quasi posterior distribution, $\tilde{\phi}_k$, respectively.

The motivation for employing these methods are threefold. First, we are able to estimate large systems that conventional Bayesian estimation methods do not permit. This is typically because the state-space representation of an N -dimensional TVP VAR (p) requires an additional $N(3/2 + N(p + 1/2))$ state equations for every additional variable. Conventional Markov Chain Monte Carlo (MCMC) methods fail to estimate larger models, which

in general confine one to (usually) fewer than 6 variables in the system. Second, the standard approach is fully parametric and requires a law of motion. This can distort inference if the true law of motion is misspecified. Third, the methods used here permit direct estimation of the VAR's time-varying covariance matrix, which has an inverse-Wishart density and is symmetric positive definite at every point in time.

In estimating the model, we use $p=2$ and a Minnesota Normal-Wishart prior with a shrinkage value $\varphi = 0.05$ and centre the coefficient on the first lag of each variable to 0.1 in each respective equation. The prior for the Wishart parameters are set following [Kadiyala and Karlsson \(1997\)](#). For each point in time, we run 500 simulations of the model to generate the (quasi) posterior distribution of parameter estimates. Note we experiment with various lag lengths, $p = \{2, 3, 4, 5\}$; shrinkage values, $\varphi = \{0.01, 0.25, 0.5\}$; and values to centre the coefficient on the first lag of each variable, $\{0, 0.05, 0.2, 0.5\}$. Network measures from these experiments are qualitatively similar. Notably, adding lags to the VAR and increasing the persistence in the prior value of the first lagged dependent variable in each equation increases computation time.

B Asset Pricing Tests

The standard Euler equation implies that the excess returns rx_{t+1}^j of a portfolio j satisfy the equation:

$$\mathbb{E}_t \left(M_{t+1} rx_{t+1}^j \right) = 0, \quad (\text{B.16})$$

in which M_{t+1} is the stochastic discount factor (SDF). We assume that the SDF is a linear function of a set of risk factors f_{t+1} and is defined as follows:

$$M_{t+1} = 1 - b'(f_{t+1} - \mu_f). \quad (\text{B.17})$$

Notice that we employ a de-meaned version of the SDF to avoid the issue related to an affine transformation of the factors ([Kan and Robotti, 2008](#)).

We are interested in testing the performance of the linear pricing models defined by Equations (B.16)-(B.17). To do so, we estimate factor loadings using the generalized method of moments (GMM) ([Hansen, 1982](#)). Substituting (B.17) into (B.16), we obtain the following N moment conditions $\mathbb{E}_t \left([1 - b'(f_{t+1} - \mu_f)] rx_{t+1} \right) = 0_N$, where rx_{t+1} is the N -

dimensional vector of test asset excess returns. We simultaneously estimate the unknown vector of factor means μ_f . Thus, GMM moment conditions also include the set of k restrictions $\mathbb{E}_t (f_{t+1} - \mu_f) = 0_k$, where k denotes the number of factors in the SDF specification. Therefore, we have the following population moment conditions:

$$\mathbb{E}_t [g_{t+1}(\theta)] = \mathbb{E}_t \begin{bmatrix} [1 - b'(f_{t+1} - \mu_f)] rx_{t+1} \\ f_{t+1} - \mu_f \end{bmatrix} = 0_{N+k},$$

where $\theta = (b', \mu')'$ is the vector of parameters. The sample moment conditions are then defined as:

$$\bar{g}_T(\theta) = \begin{bmatrix} \bar{g}_T^1(\theta) \\ \bar{g}_T^2(\theta) \end{bmatrix} = \begin{bmatrix} \frac{1}{T} \sum_{t=1}^T [1 - b'(f_{t+1} - \mu_f)] rx_{t+1} \\ \frac{1}{T} \sum_{t=1}^T [f_{t+1} - \mu_f] \end{bmatrix}.$$

We implement a one-stage GMM estimation with the prespecified weighting matrix consisting of the identity matrix I_N for the first moment conditions and a large weight assigned to the remaining restrictions. Standard errors are computed based on a heteroscedasticity and autocorrelation consistent (HAC) estimate of the long-run covariance matrix $S = \sum_{j=-\infty}^{\infty} \mathbb{E}[g(\theta)g(\theta)']$ by the [Newey and West \(1987\)](#) procedure with [Andrews \(1991\)](#) optimal lag selection.

We now evaluate the performance of linear pricing models in explaining the cross-section of network portfolios. We construct the cross-sectional R^2 , root mean squared pricing error (RMSE), and the [Hansen and Jagannathan \(1997\)](#) distance (HJ_{dist}). [Hansen and Jagannathan \(1997\)](#) provide two nice illustrations of HJ_{dist} . First, it is the maximum pricing error of a portfolio with a unit second moment. Second, it measures the minimum distance between the proposed SDF and the set of admissible SDFs. Thus, tests of the linear SDFs defined by Equation (B.17) boil down to testing the null hypothesis that the pricing errors equal zero, i.e. HJ_{dist} equals zero. Formally, the [Hansen and Jagannathan \(1997\)](#) distance is defined as:

$$HJ_{\text{dist}} = \sqrt{\min_{\theta} \bar{g}_T(\theta)' G_T^{-1} \bar{g}_T(\theta)}, \quad (\text{B.18})$$

in which G_T is the sample second moment matrix of the test excess returns, that is, $G_T = \frac{1}{T} \sum_{t=1}^T rx_{t+1} rx_{t+1}'$. One can obtain HJ_{dist} by applying the one-stage GMM estimation with the

weighting matrix equal to G_T^{-1} . The advantage of this definition is that G_T^{-1} is independent of the optimal parameters and hence this allows the comparison between different SDF specifications (Hansen and Jagannathan, 1997). The disadvantage of this approach is that G_T^{-1} is not optimal in the sense of Hansen (1982) and hence HJ_{dist} is not asymptotically a random variable of $\chi^2(N - k)$ distribution. Instead, the sample HJ_{dist} follows a weighted sum of $\chi^2(1)$ random variables (see Jagannathan and Wang (1996) and Kan and Robotti (2008) for specification tests using gross and excess returns, respectively). Therefore, we calculate the simulated p-values for HJ_{dist} based on this statistic.

C Transaction Costs

We use time-varying quoted bid-ask spreads to compute the currency excess returns adjusted for transaction costs. Following Menkhoff, Sarno, Schmeling, and Schrimpf (2012b), we take into account the whole cycle of each currency in the short or long positions from $t - 1$ to $t + 1$. When the investor buys the currency at time t and sells at time $t + 1$, he pays the corresponding bid-ask costs each period. In our notations, the excess returns of long (l) and short (s) positions are respectively $rx_{t+1}^l = f_t^b - s_{t+1}^a$ and $rx_{t+1}^s = -f_t^a + s_{t+1}^b$. If the investor buys the currency at time t but decides to keep it in the portfolio at time $t + 1$, then the net excess returns are computed as $rx_{t+1}^l = f_t^b - s_{t+1}$ and $rx_{t+1}^s = -f_t^a + s_{t+1}$. If the currency, which belongs to the portfolio at time t and is sold at time $t + 1$, was already in the current portfolio at time $t - 1$, then the excess returns $rx_{t+1}^l = f_t^b - s_{t+1}^a$ and $rx_{t+1}^s = -f_t^a + s_{t+1}^b$, that is, the investor still must initiate a position in the one-month forward contract. At the start (January 1996) and at the end (December 2013) of the sample, the investor is assumed to start and close positions in all foreign currencies.